SYNTHESIS OF COMPLIANT BISTABLE FOUR-LINK MECHANISMS FOR TWO POSITIONS

A THESIS SUBMITTED TO
THE GRADUATE SCHOOL OF NATURAL AND APPLIED SCIENCES
OF
MIDDLE EAST TECHNICAL UNIVERSITY

BY

LEVENT SUBAŞI

IN PARTIAL FULFILLMENT OF THE REQUIREMENTS
FOR
THE DEGREE OF MASTER OF SCIENCE
IN
MECHANICAL ENGINEERING

NOVEMBER 2005

Approval of the Graduate School of Natural and Applied Sciences

_____

Prof. Dr. Canan ÖZGEN

I certify that this thesis satisfies all the requirements as a thesis for the degree of Master of Science

_____

Prof. Dr. Kemal İDER
Head of Department

This is to certify that we have read this thesis and that in our opinion it is fully adequate, in scope and quality, as a thesis for the degree of Master of Science

_____

Prof. Dr. Eres SÖYLEMEZ
Supervisor

Examining Committee Members

Prof. Dr. Kemal İDER	(METU, ME)	_____
Prof. Dr. Eres SÖYLEMEZ	(METU, ME)	_____
Prof. Dr. Kemal ÖZGÖREN	(METU, ME)	_____
Asst. Prof. Ergin TÖNÜK	(METU, ME)	_____
Prof. Dr. Yavuz YAMAN	(METU, AEE)	_____

I hereby declare that all information in this document has been obtained and presented in accordance with academic rules and ethical conduct. I also declare that, as required by these rules and conduct, I have fully cited and referenced all material and results that are not original to this work.

Name, Last Name: Levent SUBAŞI

Signature :

ABSTRACT

SYNTHESIS OF COMPLIANT BISTABLE FOUR-LINK MECHANISMS FOR TWO POSITIONS

Subaşı, Levent
M.S, Department of Mechanical Engineering
Supervisor: Prof.Dr. Eres SÖYLEMEZ

November 2005, 77 pages

The aim of this study is to present a design approach for compliant bistable four-link mechanisms. The design constraints are the two positions of the mechanism, the force required to snap between the positions and the fatigue life of the designed mechanism. The theory presented here will be applied to the door lock mechanism used in commercial dishwashers, which is originally designed as a rigid inverted slider crank mechanism snapping between two positions with the force applied by a spring. The mechanism is re-designed as a compliant bistable four-link mechanism and a prototype has been manufactured.

Keywords: Compliant mechanism, Bistable mechanism, Four-bar mechanism, Pseudo-rigid-body model.

ÖZ

ÇİFT POZİSYONLU ESNEK DÖRT UZUVLU MEKANİZMALARIN İKİ POZİSYONA GÖRE SENTEZİ

Subaşı, Levent
Yüksek Lisans, Makina Mühendisliği Bölümü
Tez Yöneticisi: Prof.Dr. Eres SÖYLEMEZ

Kasım 2005, 77 sayfa

Bu çalışmanın amacı, çift pozisyonlu esnek dört uzuvlu mekanizmalar için bir tasarım yaklaşımı sunmaktır. Tasarım girdileri, mekanizmanın iki pozisyonu, pozisyonlar arasında geçiş için gereken kuvvet ve mekanizmanın ömrüdür. Burada sunulan teori, bulaşık makinelerinde kullanılan kapı kilidi parçasına uyarlanacaktır. Mevcut tasarımda bu mekanizma, yayla iki konuma sabitlenen, rijit uzuvlardan oluşan bir kol-kızak mekanizmasıdır. Mekanizma çift pozisyonlu esnek dört uzuvlu bir mekanizma olarak yeniden tasarlanmış ve prototip bir parça üretilmiştir.

Anahtar kelimeler: Esnek mekanizma, Çift pozisyonlu mekanizma, Dört uzuvlu mekanizma, Katımsı cisim modeli.

TABLE OF CONTENTS

CHAPTER 1

LITERATURE SURVEY

In this chapter, general definition and classification of compliant mechanisms is presented. Previous work on design and analysis methods is discussed. Some design software dedicated to compliant mechanisms are also presented.

1.1 Compliant Mechanisms

1.1.1 Definition

Compliant mechanisms are flexible link mechanisms, which gain some or all of their motion through the deflection of flexible members [12]. These mechanisms can be fully compliant or partially compliant. A fully compliant mechanism is one that has no rigid body joints. A partially compliant mechanism is one that has some compliant members and some non-compliant joints [16].

1.1.2 Historical Background

Mother Nature has used compliance since the beginnings of life in things such as plants, bird wings and legs of small insects. Inventors, inspiring from nature, have used deflections in their mechanism designs. For example, bows (Figure 1.1) and catapults rely on the energy stored in a deflected beam to propel their missiles across long distances. Tweezers grasp small objects between two flexible beams. Various types of springs and some hinges also use deflections to achieve the motion desired. However, scientific study of large-deflection mechanisms came much later [3].

Figure 1.1: Historical longbow

Euler was the first to quantify the deflection of flexible beams with the development of the Bernoulli-Euler equation in 1744. This equation, later, was solved for large deflections of cantilever beams using elliptical integrals. However, these solutions had very limited applications and were difficult to use. Further research in this area performed has included finding large deflections of beams with various geometries and developing methods of large-deflection finite element analysis. Hill and Midha and Her also addressed the numerical analysis of large-deflection beams [3],[16].

Semi-graphical methods are presented to be used for compliant mechanism synthesis. Compliant mechanisms using compliant segments with both end forces and end moments are investigated, along with three-dimensional compliant mechanisms. Optimization to the design of compliant mechanisms is also introduced. The effects of compliant members on mechanical advantage in a mechanism have also been investigated later. A system of classification and nomenclature for compliant mechanisms has also been established to aid in the naming and analysis of compliant mechanisms in 1994 [3].

Howell and Midha introduced the idea of a pseudo-rigid-body model to simplify compliant mechanism analysis [3]. In this model, a flexible mechanism link is modeled as two or more rigid links joined by pin joints. A presentation of a pseudo-rigid-body model for many types of flexible links was presented in the following years. This model allows many compliant mechanisms to be designed and analyzed much more easily than was previously possible.

In recent years, work has focused on methods of synthesizing new compliant mechanisms. Ananthasuresh presented work done on applying topological synthesis to the design of compliant mechanisms in 1994 [22]. In this method, a computer-driven optimization routine attempts to find the right configuration of flexible material to accomplish a certain task.

1.1.3 Advantages of Compliant Mechanisms

An advantage of compliant mechanisms is the reduction in the total number of parts required to accomplish a certain task. This reduces manufacturing and assembly time and cost [2]. Some mechanisms may even be constructed of one piece. This kind of design has been given a new name recently, which is “Design for no assembly” (DNA). Virtually, any product with multiple mechanical parts performing a motion function can be considered for a no-assembly design approach utilizing compliant mechanisms [17]. In Figure 1.2, a windshield wiper design made by FlexSys Inc. can be seen. The top image shows a 15 piece conventional wiper, and the bottom shows a single-piece compliant wiper design that can be injection molded in one-step. The advantage of this wiper is that, it evenly distributes blade pressure and can conform to any windshield, from flat to highly curved [18].

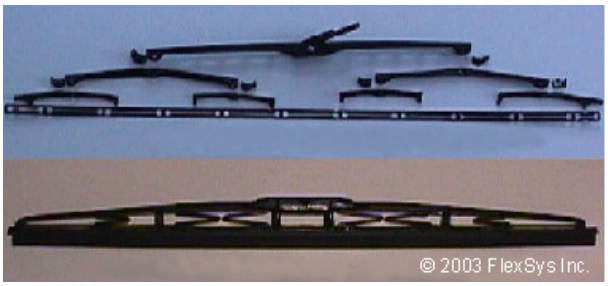

Figure 1.2: Windshield wiper [18]

Since compliant mechanisms have fewer movable joints, need for lubrication is less. Also because of that, mechanism precision is increased and vibration, noise and backlash may also be reduced.

Because of the fact that compliant mechanisms are made up of flexible members, the deflection of these members can be used as an advantage during design. For example, constant force mechanisms can be designed.

Weight issue is generally significant in some applications, such as aerospace. Compliant mechanisms are lighter than rigid link mechanisms synthesised for the same purpose.

Another advantage of compliant mechanisms is the ease with which they are miniaturized. Simple microstructures, actuators and sensors are widely used in MEMS applications [2].

1.1.4 Challanges of Compliant Mechanisms

The main disadvantage of compliant mechanisms is the difficulty of analyzing and designing them. Knowledge of mechanism analysis and synthesis methods and the deflection of flexible members is required. It is necessary to understand the interactions between “mechanism theory” and “strength of materials”, in a

complex situation. Some theory has been developed to simplify this problem. It is important to learn these new advances to overcome the limitations.

Fatigue analysis is another issue. Since compliant segments are often loaded cyclically, those members must be designed to have sufficient fatigue life to perform their prescribed functions.

Energy storage of the flexible members can be a disadvantage for some mechanisms. For example, if mechanism's task is to transfer energy from input to output, not all of input energy is transferred, but some is stored in the mechanism.

The motion from the deflection of compliant links is also limited by the strength of the deflecting members. Furthermore, a compliant link cannot produce a continuous rotational motion which is possible with a pin joint.

Compliant links that remain under stress for long periods of time or at high temperatures may experience stress relaxation or creep [2].

1.2 Compliant Bistable Mechanisms

Bistable mechanical devices remain stable in two distinct positions without power input. They find application in valves, switches, closures, and clasps. Figure 1.3 is an example of a fully compliant bistable switch as fabricated (a) and closed (b).

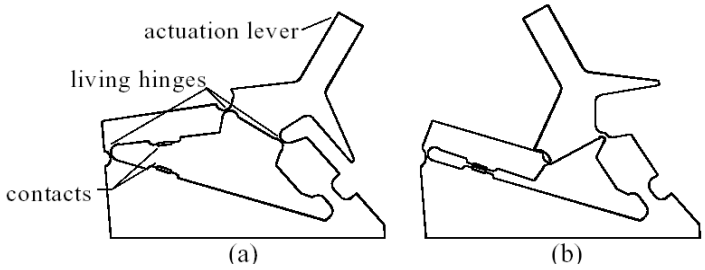

Figure 1.3: Example of a compliant bistable switch [2]

Mechanically bistable behavior results from the storage and release of energy, typically in springs, with stable positions occurring at local minima of stored energy. Compliant mechanisms offer an elegant way to achieve this behavior by incorporating both motion and energy storage into the same flexible element.

Compliance in bistable mechanisms offers several advantages, such as reduction in part-count, reduced friction, and less backlash and wear. However, the design of compliant bistable mechanisms is often not straight-forward or easy, requiring the simultaneous analysis of both the motion and energy storage of the mechanism.

Design methods found in literature, depend on the analysis of a previously synthesised mechanism and finding two stable positions for that mechanism in most cases. There is not a straightforward method presented for two position synthesis or a method regarding force requirements.

1.3 Compliant MEMS

1.3.1 Definition and Fabrication

Micro-electro-mechanical systems (MEMS) integrate electrical circuitry with mechanical devices having dimensions measured in microns [16]. Several methods of MEMS fabrication exist. The most common one is surface micromachining. Surface micromachining takes place on a silicon wafer using techniques similar to those used for integrated circuit manufacturing [2].

1.3.2 History of Compliant MEMS

Although many researchers have used deflections to gain motion, some have specifically studied the use of deflection in MEMS. Ananthasuresh applied

topological synthesis to the design of compliant MEMS [22]. He described the principal benefits and challenges. Some examples of design of compliant MEMS using the topological syntehsis method and pseudo-rigid-body models can be found in literature [3].

1.3.3 Advantages and Challanges of Compliance in MEMS

The advantages of compliance in MEMS [2] are that, compliant mechanisms:

- Can be fabricated in a plane
- Require no assembly
- Require less space and are less complex
- Have less need for lubrication
- Have reduced friction and wear
- Have less clearance due to pin joints, resulting in higher precision
- Integrate energy storage elements (springs) with the other components

There are also some challanges associated with designing compliant MEMS. The performance is highly dependent on the material properties, yet the design is limited to a few materials that are compatible with the fabrication methods. Also, the fabrication method itself creates some problems. For example, “stiction” occurs in surface micromachining. The machined structure remains stuck to the substrate and large force is necessary to move it [3].

1.3.4 Bistable MEMS

Currently, studies are being done to investigate the usefulness of bistable mechanisms on the micro-level as valves and switches. A design of bistable mechanism developed at Brigham Young University can be seen in Figure 1.4, at its open and closed positions. This MEMS bistable mechanism has been actuated by the Thermomechanical In-Plane Microactuator (TIM) [19].

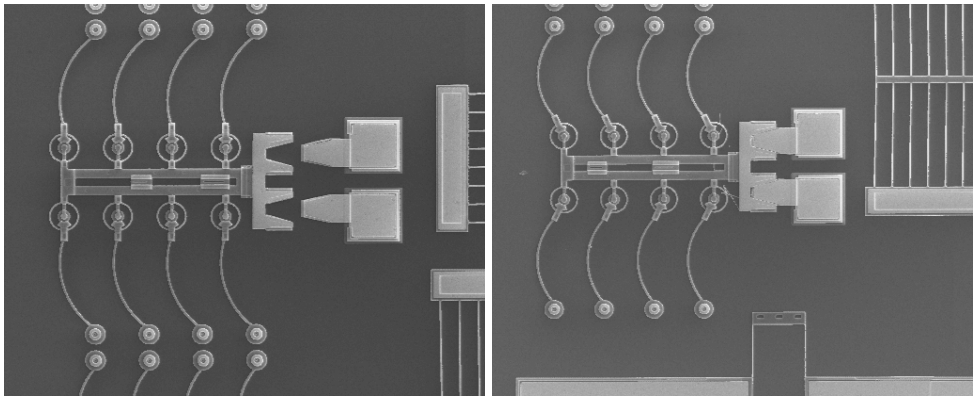

Figure 1.4: Example of a bistable mechanism in MEMS applications [19]

Bistable MEMS could perform switching or positioning operations without the need of a continual energy input. This advantage of bistable mechanisms should allow a large savings in energy for many MEMS applications. Bistable MEMS would also make applications possible which are not feasible otherwise. For example, a bistable mechanism could act as a non-volatile memory cell, allowing memory storage without the need of continual energy input. Some researchers have recognized these possible advantages, and several examples of simple bistable MEMS have been built and tested.

1.4 Design Methods

1.4.1 The Pseudo-Rigid-Body Model

In pseudo-rigid-body model, flexible links are replaced by rigid links and rotational springs corresponding to the bending of these links.

Consider the flexible beam shown in Figure 1.5. The beam end deflection path under a vertical load, as predicted by elliptic integral solutions, is shown. It is seen that the path is nearly circular, allowing it to be approximated by a rigid

beam connected to a pin joint at the center of the deflection path. This model may be drawn as shown in Figure 1.6. In the model, the rigid, rotating beam is of length $\gamma\ell$ – the "characteristic radius" - where ℓ is the length of the flexible beam and γ is a parameter known as the "characteristic radius factor." The beam's resistance to bending is modeled by a torsional spring placed at the pin joint [2].

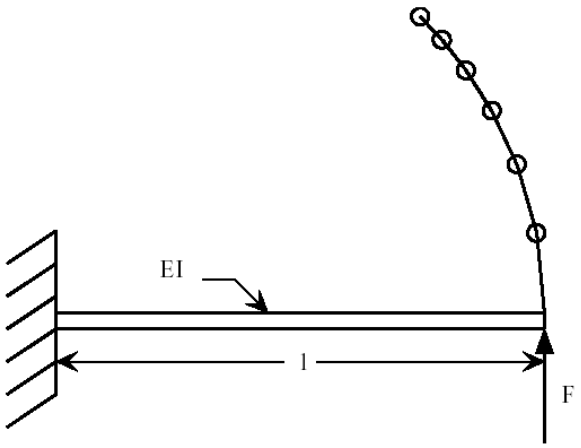

Figure 1.5: Fixed flexible beam with an end force [19]

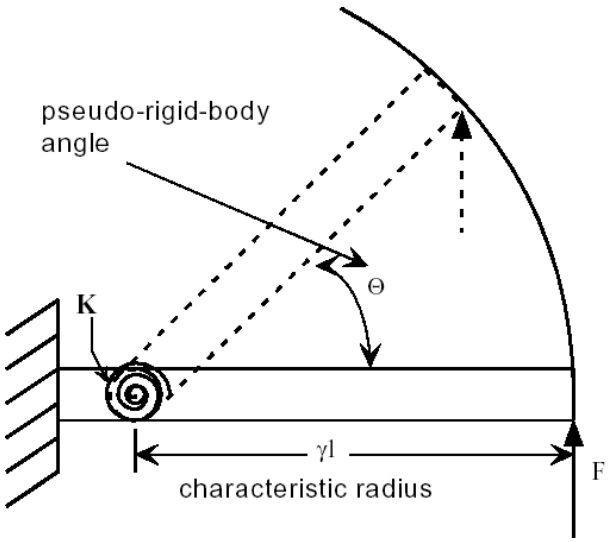

Figure 1.6: Pseudo-rigid-body model of a flexible beam with an end force [19]

A pseudo-rigid-body model has also been developed for a small-length flexural pivot, as shown in Figure 1.7. Because the thin flexible segment is much shorter than the rigid segment it attaches to, it may be modeled with a pin joint in the center of the pivot, as shown in Figure 1.8 [2].

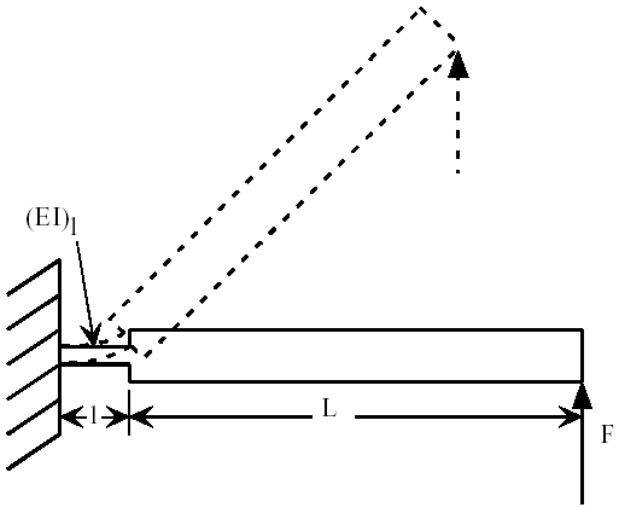

Figure 1.7: Small-length flexural pivot with an end force [2]

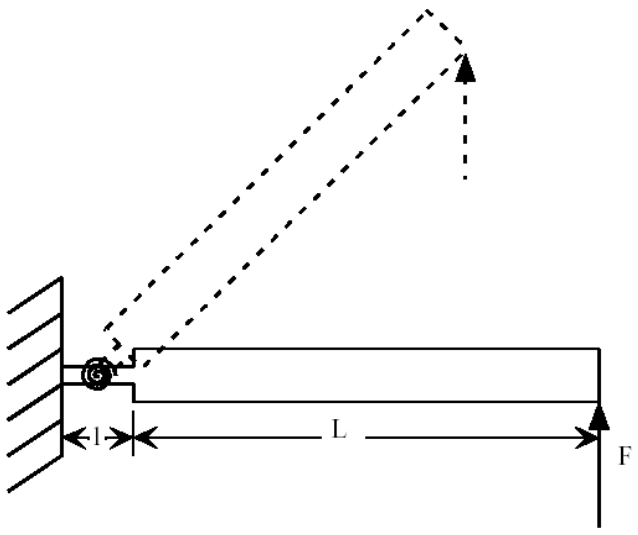

Figure 1.8: Pseudo-rigid-body model of a small-length flexural pivot [2]

A living hinge is another case of small length flexural pivots. It is a very short, very thin pivot. Because of its small stiffness compared to other segments usually found in a compliant mechanism, it is often represented simply by a pin joint, with no torsional spring.

The fixed-guided segment shown in Figure 1.9 also has a corresponding model. This segment has a moving end which is constrained to remain parallel to its original direction at every instant. The combination of force and moment at the moving end create a moment distribution which is always zero at the center of the beam. Hence, this segment may be modeled as two cantilever beams with forces at the free ends. Placing the beams end to end results in a pseudo-rigid-body model like that shown in Figure 1.10 [2].

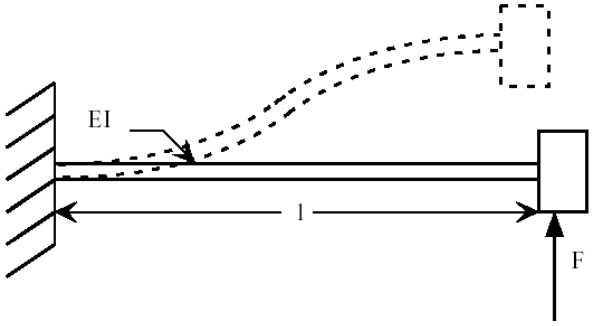

Figure 1.9: Fixed-guided beam [2]

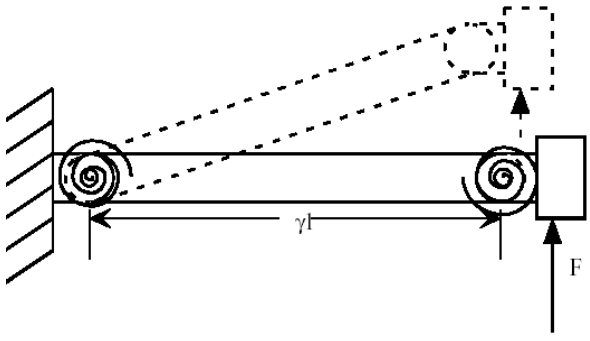

Figure 1.10: Pseudo-rigid-body model of a fixed-guided segment [2]

The pseudo-rigid-body model works very well in many situations, but it has several limitations. It is very accurate over fairly large deflections, but it begins to lose accuracy if the deflection angle becomes too high. Maximum deflection angles are tabulated for keeping the deflection error under 0.5% [2]. Also, when using this model, it must be kept in mind that the joint does not allow full rotation.

1.4.2 Topology Synthesis and Optimization

The goal of topology synthesis is to identify the optimum number and connectivity of structural elements to achieve specified motion requirements. Topology synthesis is a critical stage of the design process, due to the fact that the main performance of a compliant system is determined by its structure configuration.

An example optimization problem is sketched in Figure 1.11 below. In the general layout optimization problem, the purpose is to find the distribution for a given amount of material for a structure supported on its boundaries and subjected to a given loading condition, such that an objective function is optimized. In this case the compliance is the objective function. The amount of material is constrained and the distribution is limited to the design domain. The design domain can have regions fixed to be solid or void.

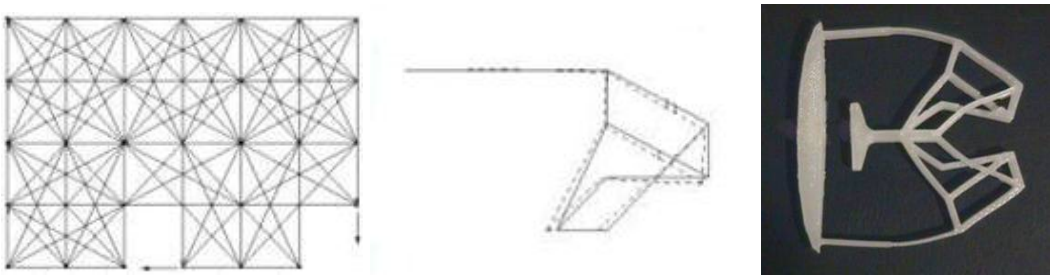

(a) (b) (c)

Figure 1.11: An example topology optimization problem [20]

The topological synthesis of compliant mechanisms is accomplished through a four-step process.

The first step is to enumerate the possible combinations of segment type (rigid or compliant) without regard to the ground segment or the type of connections between segments. After the possible segment combinations have been enumerated, the design requirements are investigated and isomorphic chains are removed from further consideration.

The second step of the topological synthesis process is to enumerate all the possible combinations of connections between segments without regard to the segment types being connected. Although, isomorphisms are not investigated after this phase of the design process, resulting compliant chains are investigated for conformance to requirements.

The third step of the topological synthesis process is to combine the results of the segment and connection-type enumeration processes. The subsequent kinematic chains are grouped by the original compliant chain from the segment enumeration process. This grouping will help limit the extend of later isomorphism investigations. The connections between segments are now examined to remove any fixed connections between rigid segments and the chains are investigated to remove any isomorphisms.

The fourth, and final, step of the topological synthesis process is to sequentially fix, or ground, each rigid segment to form mechanisms. If more than one mechanism is formed from a particular compliant chain, the mechanisms formed from that chain need to be investigated to ensure that they are unique (nonisomorphic).

As with all the steps of the topological synthesis process, the applicable design requirements are enforced. The resulting mechanisms are forwarded for further

investigation, which may include a topological analysis or ranking to determine which mechanisms will be selected for a particular application [20].

1.4.3 Type Synthesis

Type synthesis may be defined as the process of determining possible mechanism structures to perform a given task or combination of tasks without regard to the dimensions of the components. Type synthesis is performed to select a mechanism type before carrying out dimensional synthesis, which is the process of choosing mechanism dimensions to create a finished mechanism design.

The first step of the design process is the formulation of a mathematical model to represent the structure of a mechanism. In rigid-body kinematics, graph theory provides a mathematically rigorous representation of a mechanism structure through the use of matrices. The matrix representation for compliant mechanisms builds on the foundation established in rigid-body kinematics by adding information regarding segment type and the connectivity between segments to the matrices that represent a mechanism's topology.

Bistable mechanisms require the use of compliant segments in such a way that the mechanism has two stable states. Conventional type synthesis techniques make no attempt to describe the energy states of the mechanism being designed. No method currently exists which allows the description of the general stability of mechanism topologies. The type synthesis technique consists of finding a number of possible mechanism configurations, including kinematic inversions of each type, which can solve the particular problem. The mechanism configuration which will most easily solve the problem can then be chosen [3].

1.5 Design Software

1.5.1 MSC ADAMS/Autoflex

ADAMS/AutoFlex can be used for flexible body simulation of a mechanical design. ADAMS/AutoFlex is useful for early simulation of the effects of flexibility in mechanical systems when detailed finite element representations aren't available. Using ADAMS/AutoFlex, one can build a parametric flexible body representation of a component, analyze the system, make changes to the flexible body and evaluate the effect of the changes [21].

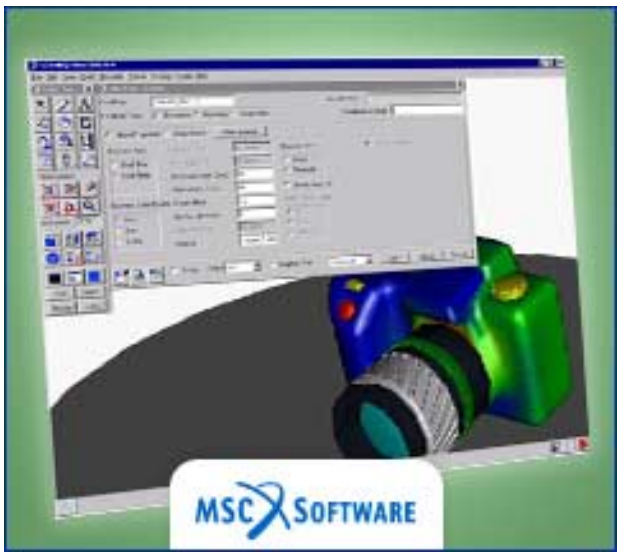

Figure 1.12: Snapshot of the MSC ADAMS/Autoflex Software [21]

1.5.2 PennSyn

PennSyn 1.0 is a software developed by the research group of Ananthasuresh, in University of Pennsylvania [22]. It is implemented in Matlab 5.3 (release 11). It has an easy-to-use menu with help buttons for each step. It generates compliant

topologies, animates the resulting motion, creates an IGES file of the solution, and stores the solution for later use.

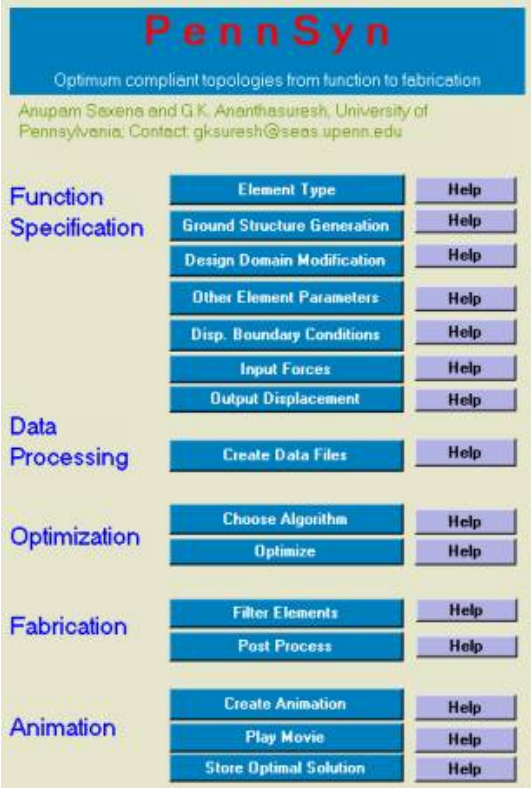

Figure 1.13: Snapshot of the PennSyn software [22]

1.5.3 TOPOPT

TOPOPT is a web-based topology optimization program developed by Dmitri Tcherniak, Ole Sigmund, Thomas A. Poulsen and Thomas Buhl [20]. The TOPOPT program solves the general topology optimization problem of distributing a given amount of material in a design domain subject to load and support conditions, such that the stiffness of the structure is maximized. The restrictions on the TOPOPT program are the following:

- Two dimensions
- Rectangular design domains
- 1000 square elements (= 1000 design variables)
- 100 design iterations

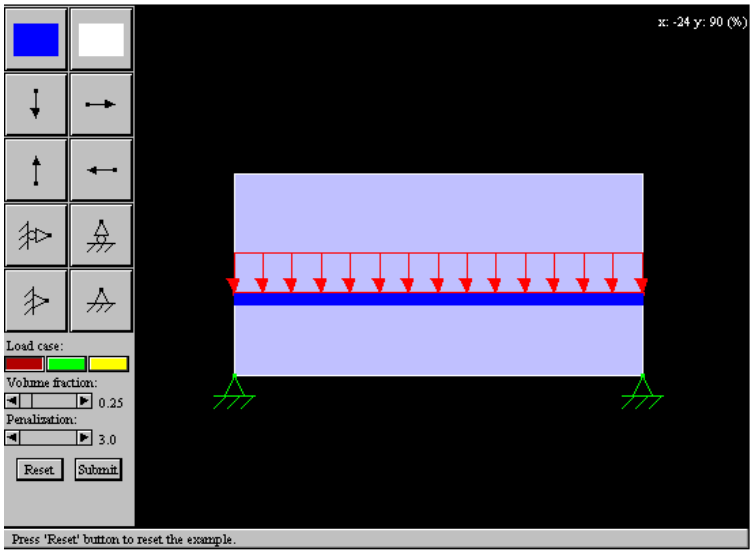

Figure 1.14: Snapshot of the TopOpt software [20]

The short-term goal of the web-based topology optimization program TOPOPT is to develop a simple-to-use topology optimization tool that can be used in the education of engineers, architects and other structural designers and to investigate the use of web-browsers as interfaces to CAD-programs.

The long-term goal is to develop an interface to a multi-purpose topology optimization program that can be used to solve general structural design problems, MEMS design problems and other topology optimization problems involving multiple physical domains [20].

1.5.4 OPTISHAPE

OPTISHAPE is a software developed by Quint Technologies [23]. It is based on the structural topology optimization using the homogenization method. This theory has been applied to the various kind of problems such as static problem, eigenvalue problem and frequency response problem.

In the optimal design of the layout (topology) of elastic structures based on the homogenization design theory, the design domain is assumed to be composed of infinitely periodic microstructures, and each microstructure has a rectangular hole as shown in Figure 1.15. The length of the sides and angle of rotation are design variables, and the size of each element hole is determined by the sensitivity of the objective function with the volume constraint and boundary conditions. Since each element hole is allowed to possess a different size and angle of rotation, uniformly distributed porous material in the initial stage will have a different size of element holes at the end of optimization as shown in the figure. Therefore, if the domain is viewed in a global sense, optimal topology is clearly seen [23].

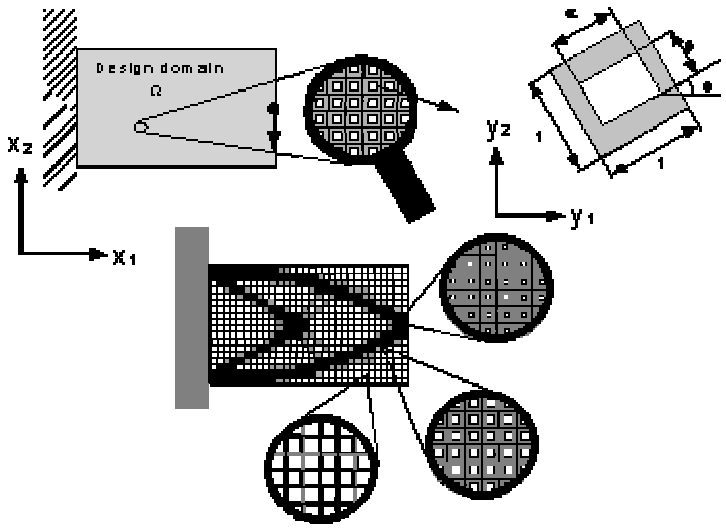

Figure 1.15: Sketch to clarify the underlying concept of Optishape software [23]

1.5.5 CSDL

In order to numerically implement the design theory, an optimization and analysis software based on Matlab platform has been developed by research students of Sridhar Kota, in University of Michigan [17].

The compliant mechanism is discretized with six degree of freedom frame finite elements. The energy efficiency of the system is maximized under the reasonable physical and geometrical boundary conditions. The specification of the mechanical advantage and geometric advantage can be reached after the convergent iterations. A promising result with great efficiency can be found if the topology and initial conditions are reasonable.

After the optimization process, dynamic analysis will be performed so that a full understanding for the performance of compliant mechanism can be achieved. The analyses include natural frequency and mode, static force analysis, dynamic responses, spectrum analysis, sensitivity analysis and equivalent spring characteristic analysis.

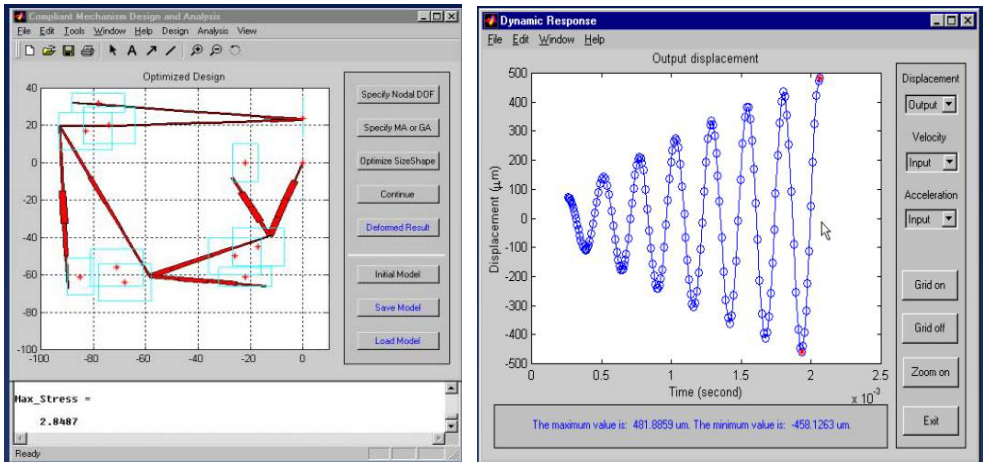

(a) (b)

Figure 1.16: Snaphots of the CSDL software [17]

CHAPTER 2

PRELIMINARY CONCEPTS

Aim of this chapter is to introduce some basic concepts, including sections on rigidity and compliance. Theory presented here will be used in the following chapter to come up with a synthesis method of compliant four-bar mechanisms.

2.1 Rigid Mechanism Theory

Synthesis of a four-bar mechanism with two positions is introduced below.

Chasles' theorem:
In Figure 2.1, a body representation is shown. Points A and B are any points chosen on the body. Notation *1* and *2* represents the two positions of the body.

The plane motion of a rigid body most simply occurs by a rotation about the "pole" which is located at the perpendicular biceptors of two pairs of homologous points A_1A_2 and B_1B_2.

Accordingly, point A rotates with respect to a point chosen on the perpendicular bicector of pair of homologous points A_1A_2. Also, point B rotates with respect to a point chosen on the perpendicular bicector of pair of homologous points B_1B_2. When the two points are chosen, a four-bar mechanism is constructed, where $\left|\,AB\,\right|$ becomes the coupler link.

$A_0A_1B_1B_0$ shows the first position of the four-bar, whereas $A_0A_2B_2B_0$ shows the second position. While performing the synthesis, A_0 and B_0 can be selected in infinitely many ways [15].

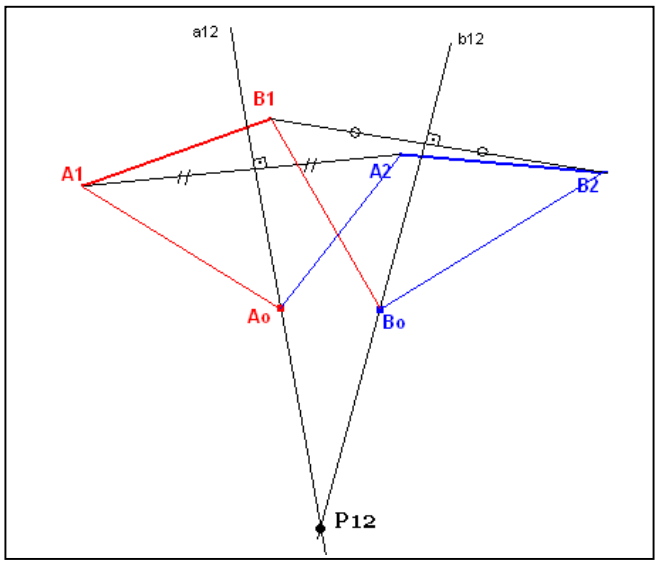

Figure 2.1: Constructed four-bar mechanism according to the two distinct positions of a body [15]

Analytical representation:

According to a fixed general frame, coordinates of the endpoints of the links can be referred as A_{1x}, A_{1y}, B_{1x}, ... and so on.

Two positions of the coupler link is the design input (coordinates of the coupler link is specified). So, it is possible to write the equation for the imaginary line a_{12}:

$$Y=m.X+D \text{ (where m is the slope)} \tag{2.1}$$

The slope of the line can be found from the slope of the imaginary line $|A_1A_2|$. Since they are perpendicular, the multiplication of the slopes gives minus one. So, slope m is found as:

$$m = \frac{A_{1x} - A_{2x}}{A_{2y} - A_{1y}} \tag{2.2}$$

Also, it is known that, line a_{12} passes from the midpoint of the line $|A_1A_2|$. The point coordinate is:

$$\frac{A_{1x}+A_{2x}}{2}, \frac{A_{1y}+A_{2y}}{2}$$

Other unknown D is found by replacing this coordinate at equation (2.1).

Since point A_0 is selected on the line a_{12}, the coordinates of A_0 are found from the equation of line a_{12}. Geometrical representation will be (A_{0x}, A_{0y}).

$$A_{0y} = \frac{A_{1x}-A_{2x}}{A_{2y}-A_{1y}} \cdot A_{0x} + \frac{A_{2y}^2 - A_{1y}^2 - A_{1x}^2 + A_{2x}^2}{2 \cdot (A_{2y}-A_{1y})} \tag{2.3}$$

Similarly, point B_0 is found as (B_{0x}, B_{0y}).

$$B_{0y} = \frac{B_{1x}-B_{2x}}{B_{2y}-B_{1y}} \cdot B_{0x} + \frac{B_{2y}^2 - B_{1y}^2 - B_{1x}^2 + B_{2x}^2}{2 \cdot (B_{2y}-B_{1y})} \tag{2.4}$$

After the four-bar is constructed according to two positions, link lengths and configurations are now known. So, for a given input variable (such as the angle of the first link with respect to ground), position analysis can be performed for the whole domain of the variable, using Freudenstein's equation [14]:

$$k_1 \cdot \cos(\theta_{14}) - k_2 \cdot \cos(\theta_{12}) + k_3 = \cos(\theta_{14} - \theta_{12}) \tag{2.5}$$

where k_i's are:

$$k_1 = \frac{a_1}{a_2}$$

$$k_2 = \frac{a_1}{a_4}$$

$$k_3 = \frac{a_1^2 + a_2^2 - a_3^2 + a_4^2}{2 \cdot a_2 \cdot a_4}$$

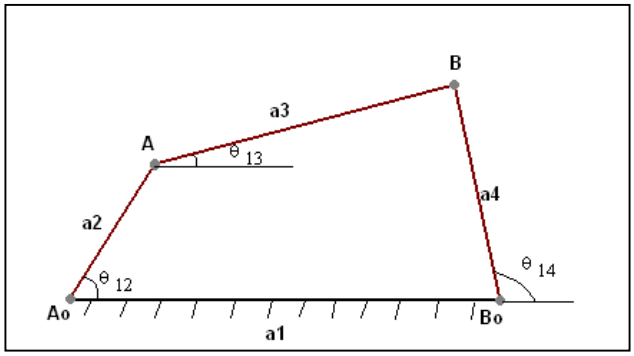

Figure 2.2: General representation of a four-bar

Although the four-bar mechanism synthesised exists at the two design positions, it may not function in between these two positions because of branching. Therefore, the resulting mechanism must be checked for movability [13].

2.2 Grashof's Criterion

In this thesis, this criterion need not be checked because of the method used in the thesis. But, it generally represents a guideline for bistable mechanism synthesis. So, it is briefly presented here.

Consider a four-bar mechanism, where symbols represent the following:

s: shortest link length
l: longest link length
p,q: other two link lengths

The mechanism is said to be a Grashof mechanism if following relation holds:

$$s+l \leq p+q \tag{2.6}$$

The mechanism is called non-Grashof otherwise.

In a Grashof mechanism, the shortest link can rotate 360^{o} with respect to any other link connected to it. In a non-Grashof mechanism no link can rotate through a full revolution [14].

If the four-bar mechanism is a Grashof mechanism, torsional spring **must** be located opposite the shortest link and when spring is undeflected, shortest and other link connected to it and opposite the spring must be non-collinear (for one spring in the system), in order to obtain bistable behaviour. If the four-bar mechanism is a non-Grashof mechanism, when spring is undeflected, two links opposite the spring must be non-collinear (for one spring in the system), in order to obtain bistable behaviour. Proof can be seen at [3].

There can be more than one spring in the system, as long as the above criterion is satisfied. For a fully compliant bistable four-bar, in all cases there exists a solution for bistability.

2.3 Stability

Stable position of a mechanism means that, for a small shift from the position, the mechanism tends to return to its undisturbed position.

Howell explains stability, by making use of "ball on the hill" analogy [2]. As seen from Figure 2.3, points A and C are stable equilibrium positions, whereas point B is an ustable equilibrium position (If a system has no acceleration, it is said to be in a state of equilibrium). Small amounts of forces acting on the ball at position A or C will result in the ball returning to its initial position. If a small amount of force acts on the ball at point B, position of the ball rapidly changes until reached a stable position. Same situation occurs for bistable mechanisms and this is called "snapping".

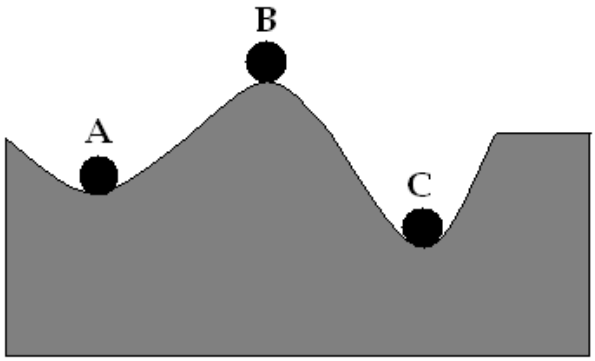

Figure 2.3: "Ball on the hill" analogy [4]

The stable equilibrium position of a system occurs at a position where the potential energy has a local minimum (Lagrange-Dirichlet theorem). Therefore, it is possible to plot the energy versus position curve and determine the stable positions of the compliant bistable mechanism, looking at the local minimums of the curve [2].

Total potential energy of a mechanism can be found by summing potential energy of each segment.

$$V_T=V_1+V_2+V_3+.... \tag{2.7}$$

For a compliant mechanism, potential energy of each segment, using pseudo-rigid-body model, is found as [8]:

$$V=\left(\frac{1}{2}\right)\cdot K\cdot \Psi^2 \tag{2.8}$$

where:
K: torsional spring constant (which is assumed to be constant)
ψ: relative deflection of the segment (pseudo-rigid-body angle)

If only one spring is present, mechanism will always have zero potential energy at both stable positions.

2.4 Pseudo Rigid Body Model of Compliant Segment Types

There are many different kinds of compliant segment types that can be modelled using pseudo rigid body model. But, especially two of them are very useful for compliant four-bar synthesis:

- Small length flexural pivots
- Fixed-pinned links

1. Small length flexural pivots:

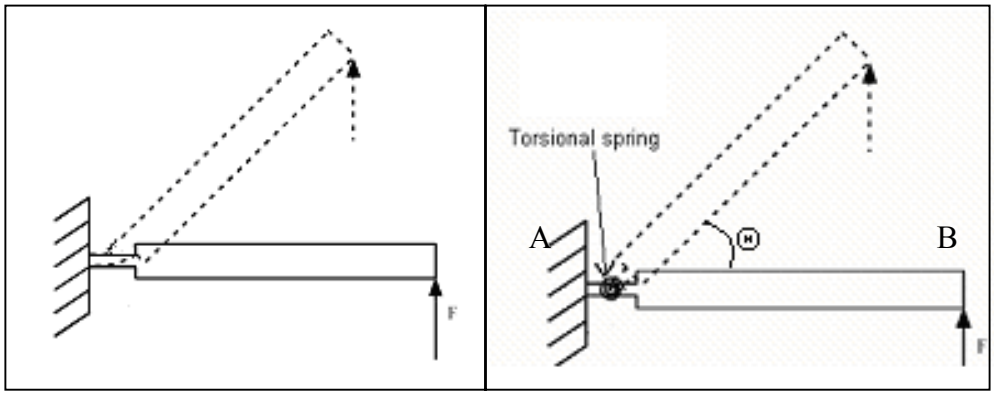

(a) (b)

Figure 2.4: Pseudo-rigid-body model of a small-length flexural pivot [3]

Figure 2.4 (a) shows a small length flexural pivot and Figure 2.4 (b) is its pseudo-rigid-body model. The torsional spring is positioned at the middle point of the small length flexural pivot (as seen in Figure 2.4b). It is a good assumption and gives enough accuracy in the calculations. Fixing the coordinate frame at point A (ground connection point), the coordinates of the endpoint of the beam (B_x,B_y) is found as [3]:

$$B_x = \left(\frac{\ell}{2}\right) + \left(L + \frac{\ell}{2}\right) \cdot \cos(\Theta) \tag{2.9}$$

$$B_y = \left(L + \frac{\ell}{2}\right) \cdot \sin(\Theta) \tag{2.10}$$

where:

ℓ: length of the flexural pivot

L: length of the link

Θ: deflection angle (pseudo rigid body angle)

The torsional spring constant, K, is found as [3]:

$$K = \frac{E \cdot I}{\ell} \tag{2.11}$$

where:

E: elasticity modulus

I: moment of inertia

2. Fixed-pinned link:

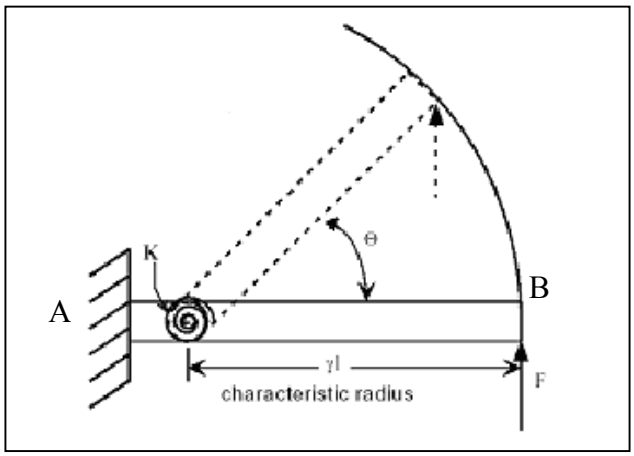

Figure 2.5: Pseudo-rigid-body model of a fixed-pinned link [3]

For a fixed-pinned segment, the torsional spring is positioned at a certain distance determined by the factor γ. Again fixing the coordinate frame at point A, endpoint coordinates of the beam (B_x,B_y) can be found as [3]:

$$B_x = L - \gamma \cdot L + \gamma \cdot L \cdot \cos(\Theta) \tag{2.12}$$

$$B_y = \gamma \cdot L \cdot \sin(\Theta) \tag{2.13}$$

The value of γ on average is 0,85, for all loading conditions [3]. The torsional spring constant for this case is approximately found as [3]:

$$K = \pi \cdot \gamma^2 \cdot \frac{E \cdot I}{L} \tag{2.14}$$

2.5 Static Failure

The compliant segment must be checked for static failure. According to distortion energy theory, effective stress σ' (also referred as von Mises stress) has to be greater than the yield strength (S_y) of the material, for static failure to occur [2].

$$\sigma' \geq S_y \quad \text{(for failure)} \tag{2.15}$$

σ' can be found by using a finite element software.

2.6 Fatigue Life Estimation

A common loading condition for compliant mechanisms is fluctuating stresses. Since most of the time, compliant segments move between undeflected and maximum deflection positions, the stress variation can be plotted as shown in Figure 2.6 [11].

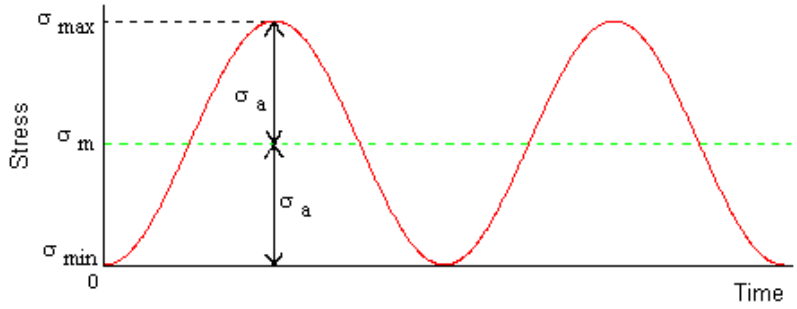

Figure 2.6: Fluctuating stress loading condition [11]

σ_m refers to mean stress and σ_a refers to alternating stress, where general equations of them are given as [11]:

$$\sigma_m = \frac{\sigma_{max} + \sigma_{min}}{2} \tag{2.16}$$

$$\sigma_a = \frac{\sigma_{max} - \sigma_{min}}{2} \tag{2.17}$$

Since $\sigma_{min}=0$ for the case shown in Figure 2.6, mean and alternating stresses can be calculated as $\sigma_m=\sigma_a=\sigma_{max}/2$.

Fatigue life of a flexible segment can be determined using *modified Goodman diagram* (Figure 2.7) [2]. Filled areas show the finite and infinite life regions.

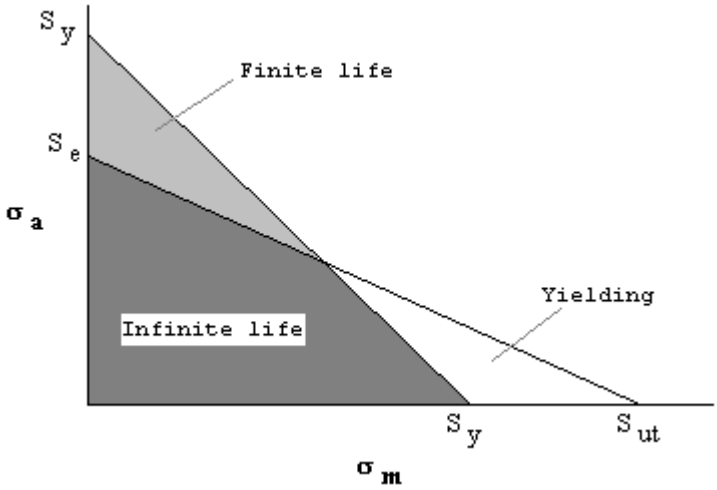

Figure 2.7: Modified Goodman Diagram [2]

S_y: Yield strength

S_{ut}: Ultimate tensile strength

S_e: Endurance limit

Line passing through S_e on σ_a axis and S_{ut} on σ_m axis, is called *modified Goodman line* and its equation is [11]:

$$\frac{\sigma_a}{S_e} + \frac{\sigma_m}{S_{ut}} = 1 \tag{2.18}$$

The safety factor for the modified Goodman line is:

$$\frac{1}{SF} = \frac{\sigma_a}{S_e} + \frac{\sigma_m}{S_{ut}} \tag{2.19}$$

For plastic parts it is recommended to use $S_e=0,2.S_{ut}$ to $S_e=0,4.S_{ut}$ [2]. Averagely $S_e=0,3.S_{ut}$ can be taken. Also taking $\sigma_m=\sigma_a=\sigma_{max}/2$ and re-arranging equation (2.19), safety factor can be calculated as:

$$SF = \frac{6 \cdot S_{ut}}{13 \cdot \sigma_{max}} \tag{2.20}$$

Infinite life generally is assumed to start from 10^6 cycles in literature for a flexible segment [11]. When safety factor is equal to one, it represents a point **on** the modified Goodman line. So, when SF=1, it corresponds to 10^6 life cycles.

For every material, there is an S-N diagram available for different loading conditions, in literature. Since they are dependent on experimental results, those diagrams should be used whenever possible. If S-N diagrams are not available, then modified Goodman method explained above can be preferred.

CHAPTER 3

DESIGN OF A COMPLIANT BISTABLE FOUR-BAR

Aim of this chapter is to introduce a design concept that can be used for two position synthesis of a compliant bistable four link mechanism. Pseudo-rigid-body model and potential energy equation corresponding to the model is used. There are analysis methods using the same concept in the literature, but they are used to define two stable positions of a constructed mechanism, whereas in this thesis, mechanism is constructed for two positions and corresponding torsional spring constants are calculated in order to realize that positions. An example is presented which uses the developed design concept.

3.1 Potential Energy Equation

Generally, in order to find stable positions of a mechanism (if position and energy equations are available), first and second derivatives of the potential energy equation with respect to input variable is used. Equating the first derivative to zero, gives the equilibrium positions. The positive magnitude of the second derivative at the equilibrium positions shows that this equilibrium position is stable [2].

The fully compliant four-bar mechanism is shown in Figure 3.1 (a). Its pseudo-rigid body model is shown in Figure 3.1 (b).

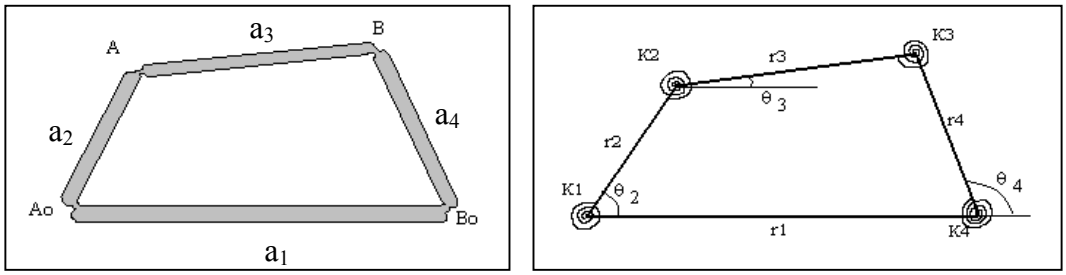

(a) (b)

Figure 3.1: Pseudo-rigid-body model of a four-bar mechanism [2]

Total potential energy equation for the mechanism is given as [2]:

$$V = \frac{1}{2} \cdot \left(K_1 \cdot \psi_1^2 + K_2 \cdot \psi_2^2 + K_3 \cdot \psi_3^2 + K_4 \cdot \psi_4^2 \right) \tag{3.1}$$

where:

$$\psi_1 = \theta_2 - \theta_{20} \tag{3.2}$$

$$\psi_2 = \left(\theta_2 - \theta_{20}\right) - \left(\theta_3 - \theta_{30}\right) \tag{3.3}$$

$$\psi_3 = \left(\theta_4 - \theta_{40}\right) - \left(\theta_3 - \theta_{30}\right) \tag{3.4}$$

$$\psi_4 = \theta_4 - \theta_{40} \tag{3.5}$$

"θ_{io}" refers to the initial (undeflected) position of the i^{th} link.

Taking the derivative with respect to the independent variable (coupler link angle θ_3 is used as the independent variable, as it will be used as the input angle later):

$$\frac{dV}{d\theta_3} = K_1 \cdot \psi_1 \cdot A_1 + K_2 \cdot \psi_2 \cdot \left(A_1 - 1\right) + K_3 \cdot \psi_3 \cdot \left(A_2 - 1\right) + K_4 \cdot \psi_4 \cdot A_2 \tag{3.6}$$

where:

$$A_1 = \frac{d\theta_2}{d\theta_3} = \frac{r_3 \cdot \sin(\theta_3 - \theta_4)}{r_2 \cdot \sin(\theta_4 - \theta_2)} \tag{3.7}$$

$$A_2 = \frac{d\theta_4}{d\theta_3} = \frac{r_3 \cdot \sin(\theta_3 - \theta_2)}{r_4 \cdot \sin(\theta_4 - \theta_2)} \tag{3.8}$$

The first derivative is actually the input torque [2]. So:

$$T_3 = \frac{dV}{d\theta_3} \tag{3.9}$$

When first derivative of the total potential energy is equated to zero, a maximum, a minimum or a saddle point is reached. The sign of the second derivative at this position determines the type of stable position. If the value of the equation is greater than zero, it represents a stable position, whereas if it is less than zero, it represents an unstable position (snapping point).

Second derivative of the total potential energy equation with respect to θ_3 can be found as:

$$\frac{d^2V}{d\theta_3^2} = K_1 \cdot \left(A_1^2 + \psi_1 \cdot A_3\right) + K_2 \cdot \left(A_3 \cdot \psi_2 + A_1^2 - 2 \cdot A_1 + 1\right) + K_3 \cdot \left(A_4 \cdot \psi_3 + A_2^2 - 2 \cdot A_2 + 1\right) + K_4 \cdot \left(A_2^2 + \psi_4 \cdot A_4\right) \tag{3.10}$$

where:

$$A_3 = \left(\frac{r_3}{r_2}\right) \cdot \left[\frac{\cos(\theta_3 - \theta_4)}{\sin(\theta_4 - \theta_2)} \cdot (1 - A_2) - \frac{\sin(\theta_3 - \theta_4) \cdot \cos(\theta_4 - \theta_2)}{\sin^2(\theta_4 - \theta_2)} \cdot (A_2 - A_1)\right] \tag{3.11}$$

$$A_4 = \left(\frac{r_3}{r_4}\right) \cdot \left[\frac{\cos(\theta_3 - \theta_2)}{\sin(\theta_4 - \theta_2)} \cdot (1 - A_1) - \frac{\sin(\theta_3 - \theta_2) \cdot \cos(\theta_4 - \theta_2)}{\sin^2(\theta_4 - \theta_2)} \cdot (A_2 - A_1)\right] \tag{3.12}$$

For a bistable compliant four-bar mechanism, the potential energy equation and its derivatives with respect to the input variable will typically be as shown in Figure 3.2.

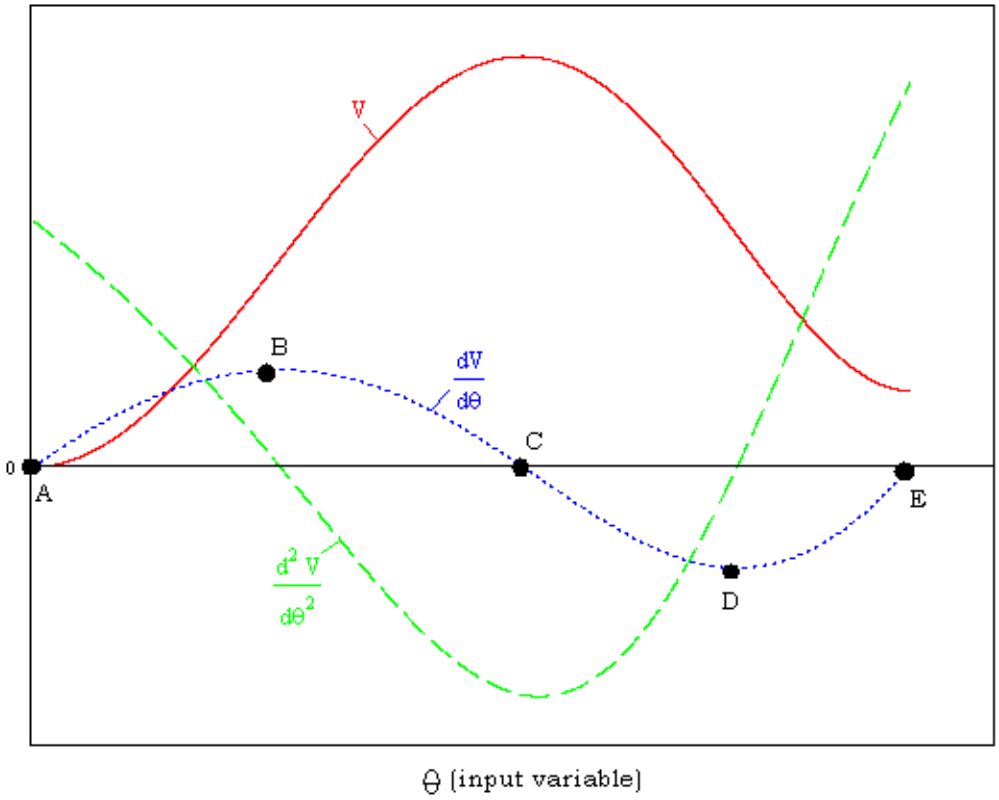

Figure 3.2: Graph of potential energy equation and its derivatives

Points A, E: Stable positions of the mechanism

Points B, D: Points at which external torque input is a local maximum for switching

Point C: Unstable position of the mechanism

For every bistable mechanism, an unstable position is also present. A bistable mechanism snaps between stable positions through the unstable position.

3.2 Design Steps

The input is the two stable positions and force required to snap the mechanism between two positions. The intend is to find the torsional spring constants as given in Pseudo-rigid-body model and corresponding dimensional properties of joints and links. Then maximum stress analysis can be performed to estimate fatigue life of the mechanism. Design steps will be realized in the next section, where an example is presented.

The basic design algorithm is:

- Deciding the number of torsional springs that is intended to be used on the mechanism.
- Deciding on the two coupler joint positions on the body.
- Choosing initial position of the input link (one of the bistable positions).
- Selecting one of the ground joint connections A_0 or B_0 (can be found by using Chasle's theorem).
- Changing the position of the other ground joint connection until input torque requirement is met (iteration step).
- Predicting the unknown torsional spring constants by making use of the derivative of the total potential energy (torque) equation.
- Choosing material for the mechanism and segment types for the joints and finding compliant joint and link dimensions.
- Checking for static failure and performing fatigue life analysis.

Regarding the design steps, it is always possible to turn back to previous steps and choose different positions or variables until all design criteria are met. For

example, choosing different number of torsional springs, choosing different coupler positions, changing the starting position, choosing different joint connections (A_0, B_0) or choosing different material or segment types is possible.

3.3 Designing a Door Lock Mechanism

Technical drawing of the door lock mechanism used in dishwashers is shown below, in Figure 3.3. It is a rigid inverted slider-crank mechanism consisting of 4 links and a spring. Design criteria for the part is:

- Two stable positions
- Force needed to snap between positions
- Fatigue life

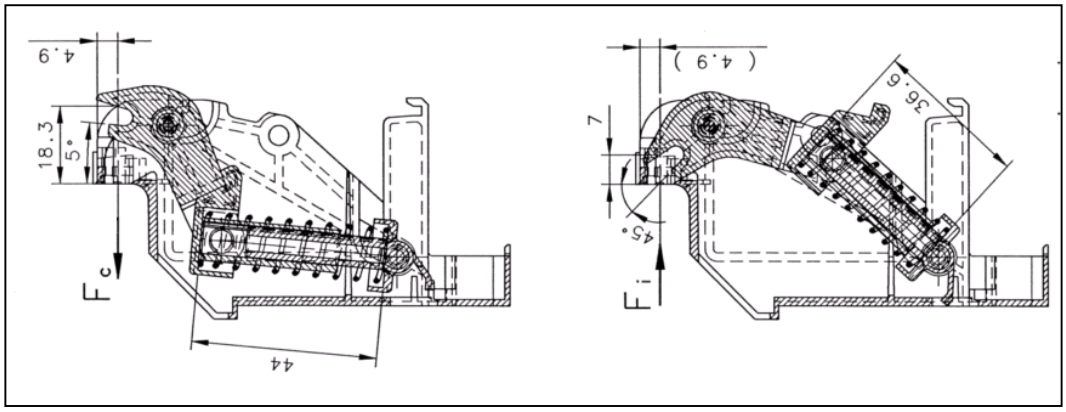

Figure 3.3: Technical drawing of door lock mechanism

The main part will be referred as *body*, and beak-like part will be referred as *beak*. The picture of the mechanism at two stable positions is shown in Figure 3.4.

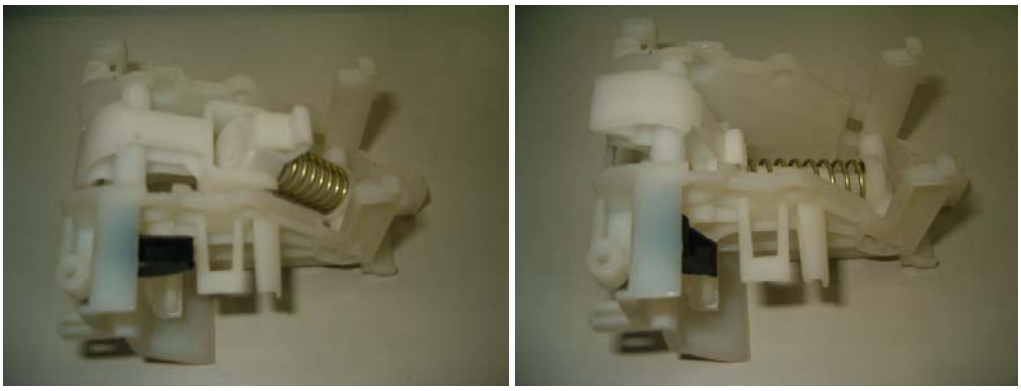

(a) (b)

Figure 3.4: Door lock mechanism at two stable positions

This mechanism can be modelled as a compliant bistable four-bar. Although design algorithm presented in Chapter 3.2 is valid for all cases, the design method slightly changes as the number of torsional spring used changes. Two cases will be presented accordingly. Design for one torsional spring will be presented first. More torsional springs will be used for the second case, respectively.

3.3.1 Design for one torsional spring

In most of the cases, designers would like to keep the design as simple as possible, as simplicity offers many advantages. In this case, designing a bistable four-link mechanism with one flexible segment (one torsional spring) can be preferred. But, it is not always possible to choose one spring, because there is a condition to it.

3.3.1.1 Deciding on the two coupler joint positions

It was mentioned in Chapter 2.3 that, for one spring in the system, the potential energy of the system is zero at both stable positions, meaning no potential energy is stored in the system at the stable positions. This necessitates the flexible link to

be **undeflected** at the stable positions. So, in order to make a design made of one torsional spring, the "pole" (as mentioned in Chapter 2.1) of the coupler has to be chosen as the flexible link's joint.

Looking at the door lock mechanism, the *beak* is the coupler link and it rotates with respect to point A, as shown in Figure 3.5. Since point A is the pole, it is chosen as one of the coupler link's joints. The other joint can be selected anywhere on the body. Point B can be chosen as the other joint for the coupler link. So, the coupler link is formed with $r_3 = |AB|$.

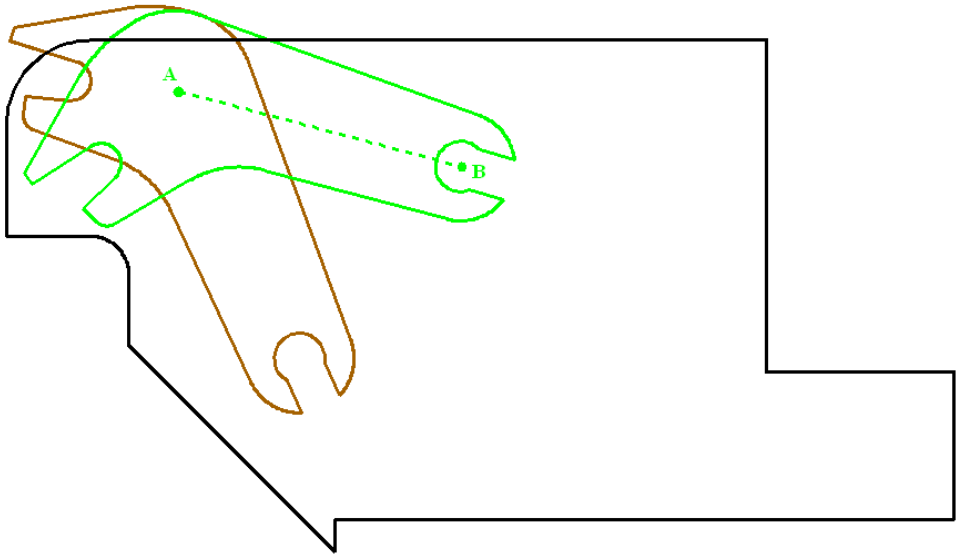

Figure 3.5: Forming the coupler link

3.3.1.2 Choosing initial position of the input link

Since flexible link returns to its undeflected position at the end of the movement, it doesn't matter which stable position of the coupler is chosen as the starting position. One of the stable positions is chosen as shown in Figure 3.6.

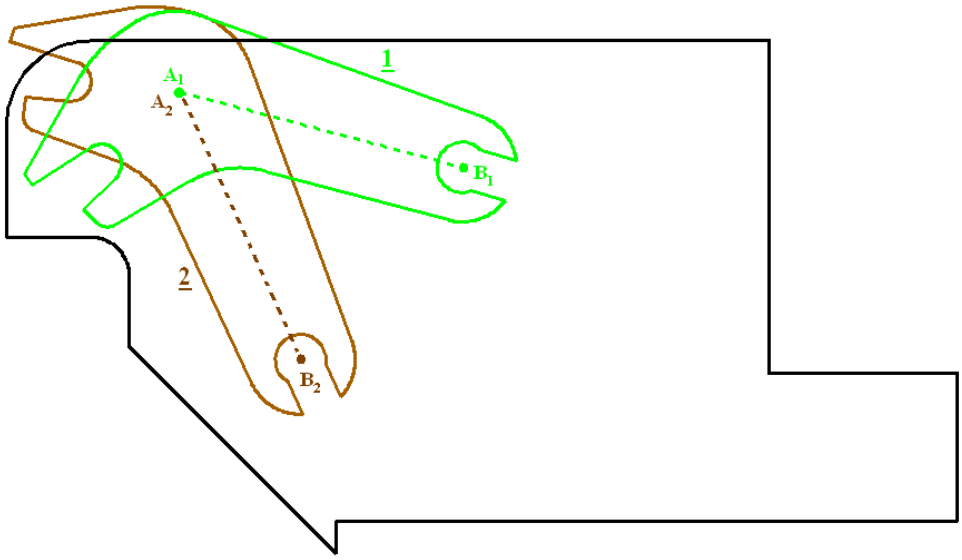

Figure 3.6: Choosing the initial position

3.3.1.3 Selecting one of the ground joint locations

There is a constraint while choosing ground joint locations. Since the mechanism works in a limited area, links are limited inside the *body's* boundary. But, it must be remembered that, during realization of the mechanism (replacing rigid links with flexible links), link lengths will elongate, so ground joints must not be on or very near the limiting boundaries.

For the four link door lock mechanism, position of the ground joint of flexible link (A_0) can be selected infinitely many ways within the body. Second link is chosen perpendicular to the *body* frame, with length $r_2 = |A_0A_1|$ (Figure 3.7).

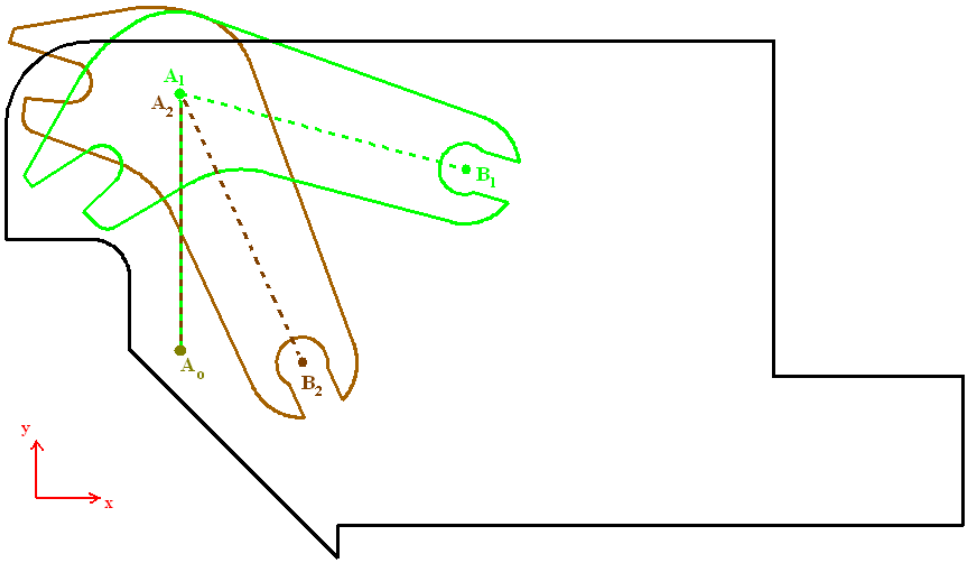

Figure 3.7: Forming the flexible link

3.3.1.4 Changing the position of the other ground joint connection

The bistable behaviour of the mechanism to be constructed is independent from K_1, the value of the torsional spring constant which is going to be located at A_0. Combining equations (3.2), (3.6), (3.7) and (3.9) (and taking $K_2=K_3=K_4=0$):

$$T_3 = K_1 \cdot \left(\theta_2 - \theta_{20}\right) \cdot \frac{r_3 \cdot \sin\left(\theta_3 - \theta_4\right)}{r_2 \cdot \sin\left(\theta_4 - \theta_2\right)} \tag{3.13}$$

At both stable positions and at the unstable position, torque will be zero. Since K_1 can't be zero, either $\theta_2=\theta_{20}$ or $\theta_3=\theta_4+k.\pi$ (where k is any integer). At the stable positions, flexible link 2 will be undeflected, so $\theta_2=\theta_{20}$ represents stable positions. At the unstable position, the potential energy of the system will reach a maximum, where link 2 has the maximum deflection. Links 3 and 4 will be collinear at this point, so $\theta_3=\theta_4+k.\pi$ represents unstable positions.

K_1 is only a scale factor that determines the maximum torque values between switching.

In order to construct a four-bar mechanism, only one varible is needed to be fixed at this point. It is the position of the other ground joint connection (B_0). When B_0 is selected; link lengths r_1 and r_4, and all angle relations can be determined. Then the mechanism is analysed between stable positions to find torque curve characteristics. So, an iteration has to be made in a certain range, until force requirements are fulfilled.

In Figure 3.8, the range of the iteration can be seen. The fixed reference frame is located at point A_0. x coordinates of B_0 can be changed starting from $x=x_s$ to $x=x_e$ and y coordinates can be calculated accordingly, so that the four-bar is constructed.

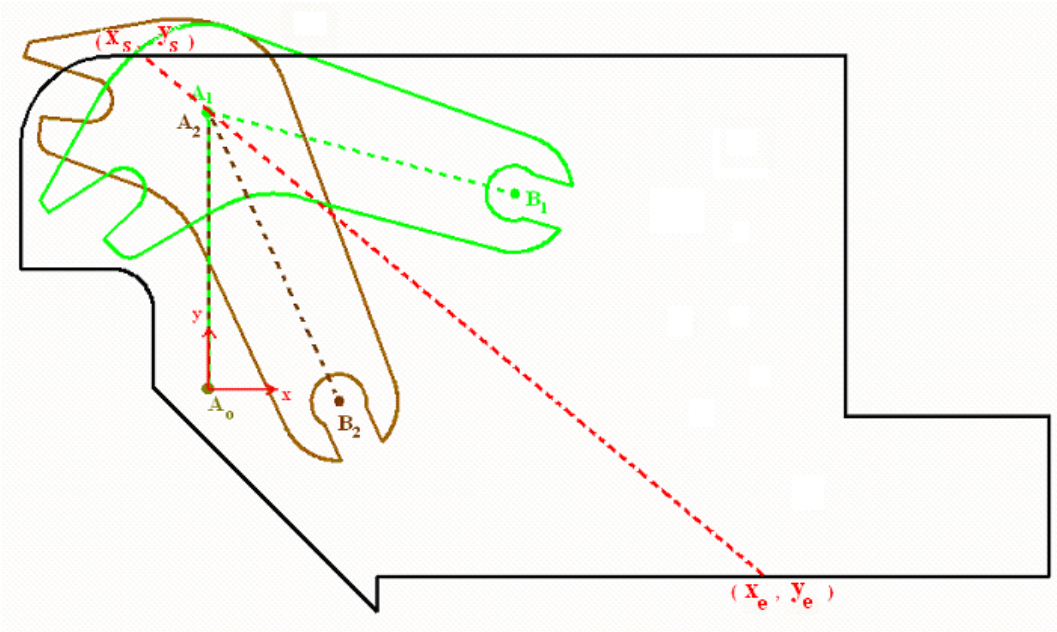

Figure 3.8: Range of iteration

Before the iteration, torque of link 3 has to be expressed in terms of force applied at the end of the beak, since force is the objective function. Also, force need not to be at a maximum where torque is maximum, so it has to be analysed seperately.

Drawing the free-body diagrams, the force and torque relation can be expressed in matrix form. Reference frame is rotated so that direction of link 1 is the x axis. So, angles shown in Figure 3.9 are taken with respect to first link, r_1 (it is important to note that, newly generated reference frame is dependent on the position of B_0).

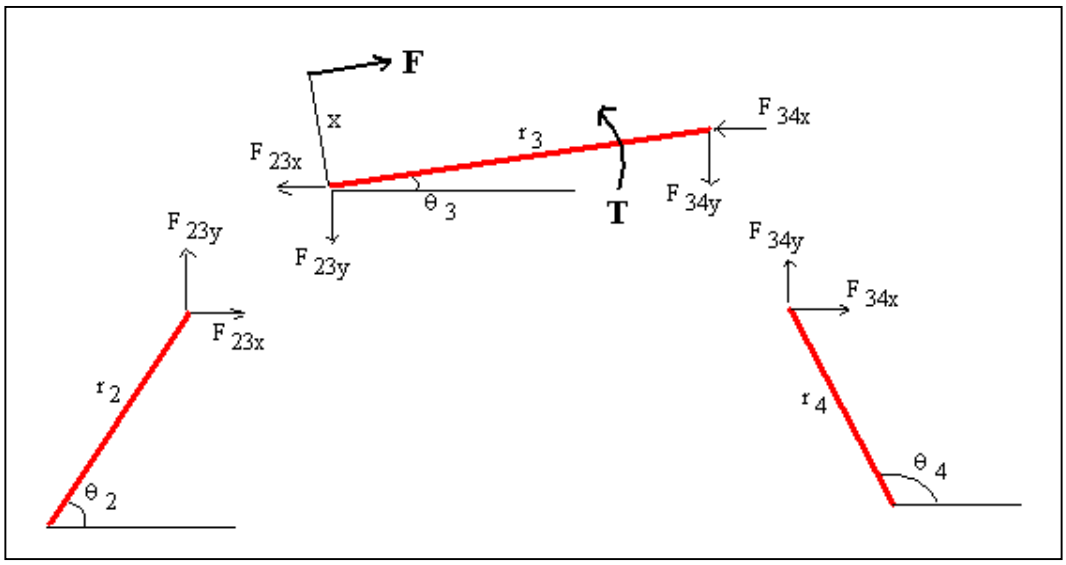

Figure 3.9: Free-body diagrams of the links

Important point is that, the direction of the force applied is independent from the position of the *beak*. It is a guided force, so whatever the angle of link 3, force is perpendicular to the **fixed** reference frame.

$$\begin{pmatrix} -r_2 \cdot \sin\theta_2 & r_2 \cdot \cos\theta_2 & 0 & 0 & 0 \\ 0 & 0 & -r_4 \cdot \sin\theta_4 & r_4 \cdot \cos\theta_4 & 0 \\ -1 & 0 & -1 & 0 & \cos(90 - \theta_1) \\ 0 & -1 & 0 & -1 & \sin(90 - \theta_1) \\ 0 & 0 & r_3 \cdot \sin\theta_3 & -r_3 \cdot \cos\theta_3 & -x \end{pmatrix} \cdot \begin{pmatrix} F_{23x} \\ F_{23y} \\ F_{34x} \\ F_{34y} \\ F \end{pmatrix} = \begin{pmatrix} 0 \\ 0 \\ 0 \\ 0 \\ -T_3 \end{pmatrix}$$

Value of F can be determined by Cramer's rule, in terms of torque, T_3.

The force requirement given in the original technical drawing is 53±10N to unlock and 28±5N to lock the door. So, the force ratio is allowed to vary between 43/33=1,303 and 63/23=2,739.

There is a direct relation between B_{0x} and the force ratio. Iteration objective is to change B_{0x} to obtain a force ratio between 1,303 and 2,739. A sample iteration routine for one torsional spring using Mathcad 2000 is presented in Appendix A. Using this routine, Table 3.1 can be filled. In the routine, a variable "i" is used instead of "x", which is transformed to vary from i=0 to i=577 (corresponding to variance $x=x_s$=-5,9 to $x=x_e$=51,8)

Table 3.1: Force ratio relationship with B_{0x}

i	ratio	i	ratio
0	1.480	300	∞
25	1.551	325	∞
50	1.637	350	-5.764
75	1.756	375	-3.094
100	1.905	400	-2.434
125	2.117	425	-2.094
150	2.460	450	-1.884
175	3.252	475	-1.741
200	∞	500	-1.638
225	∞	525	-1.559
250	∞	550	-1.498
275	∞	575	-1.448

"-" signs in the table designates that locking force is greater than unlocking force. Between i=175 and i=350, input torque tends to go to infinity, so it is not possible to define a ratio.

Since it is required to have a larger unlocking force and also looking at the ratio allowed, a value between i=0 and i=150 can be chosen.

i=150 is chosen because of the reasons that will be discussed in Chapter 4. The force graph (identical to torque graph) is shown in Figure 3.10 (value of K_1 is taken to be unit value yet).

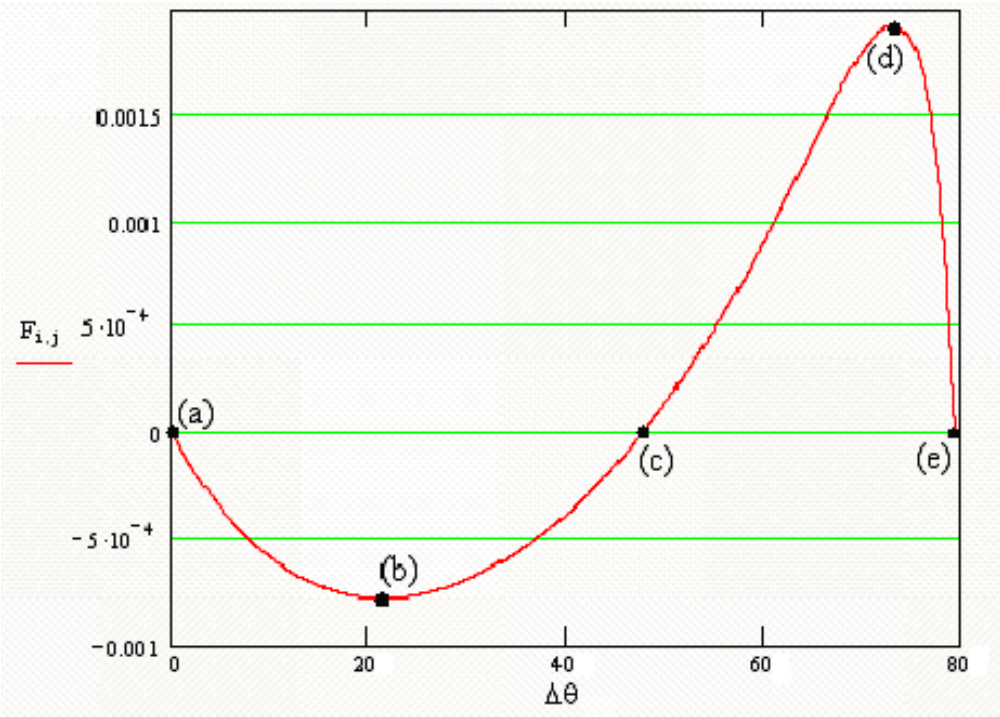

Figure 3.10: Graph of force versus rotation

The five motion phases of the mechanism is shown in Figure 3.11:

(a): Initial position

(b): Position at which force is a maximum for locking

(c): Unstable position

(d): Position at which force is a maximum for unlocking

(e): Second stable position

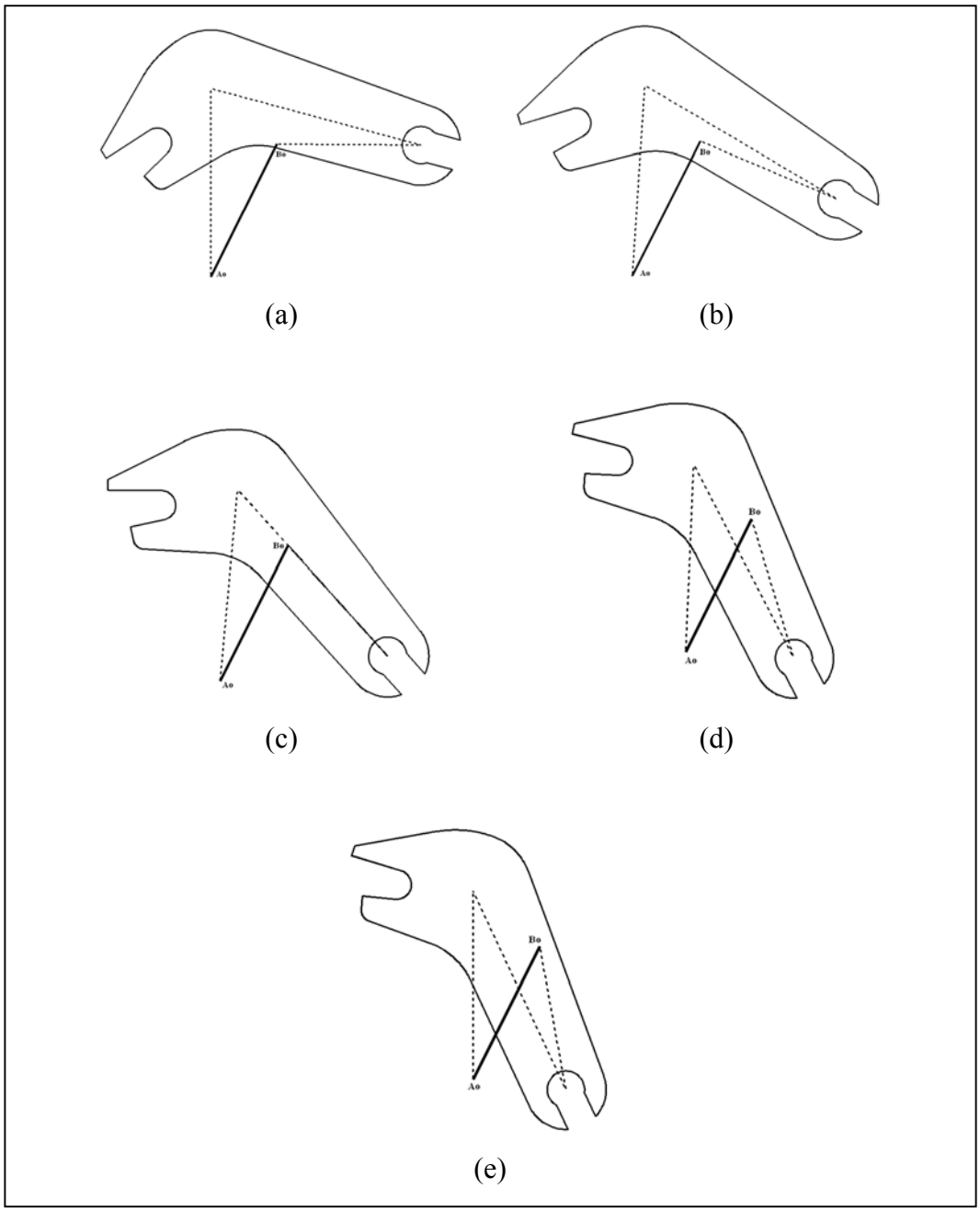

Figure 3.11: Five motion phases of the constructed four-bar mechanism

3.3.1.5 Predicting the value of the torsional spring constant

Maximum force to lock and unlock the mechanism is known in terms of K_1. When K_1 is taken as unit value, $F_{lock\text{-}max}$ and $F_{unlock\text{-}max}$ can be calculated as (also seen from the graph shown in Figure 3.10):

$F_{lock\text{-}max} = 7.83 \times 10^{-4}$ N
$F_{unlock\text{-}max} = 19.27 \times 10^{-4}$ N

Value of K_1 is directly proportional to these forces, as seen from equation (3.13) and the matrix equation. If K_1=32000 N.mm is chosen then the forces become:

$F_{lock\text{-}max} = 25.06$ N
$F_{unlock\text{-}max} = 61.65$ N

which are acceptable according to the given force tolerances at the technical drawing shown in Figure A.1.

3.3.1.6 Realizing the mechanism

Since necessary parameters are calculated, it is possible to build the mechanism with compliant segments. The material of the mechanism is chosen to be polyoxymethylene, POM (Delrin). Its Young's modulus is E=2300 N/mm^2. Material properties of some commercially available materials are listed in Appendix C.

Segment type will be chosen for the link that have the torsional spring. There are two important rules to remember while constructing the mechanism:

1. In pseudo-rigid-body model, when switching from rigid mechanism with torsional springs to actual mechanism, lengths of the flexible links differ.

2. As the pseudo-rigid-body model theory is about compliant segments that are perpendicular to connections, the links must be formed so that they are always perpendicular to its connectors (whether fixed or not).

For the constructed door lock mechanism, link 2 can be chosen as a small-length-flexural pivot or a fixed-pinned link. Fixed-pinned link has generally better fatigue resistance than small-length-flexural pivot, so it can be chosen.

Assuming a rectangular cross-section for the link, from equation (2.14):

$$K_1 = \pi \cdot \gamma^2 \cdot \frac{E \cdot \left(\frac{1}{12} \cdot b \cdot h^3 \right)}{L} \tag{3.14}$$

where:
L: length of the actual link
b: thickness of the joint (inside the plane)
h: width of the link
γ: characteristic radius factor

According to Pseudo-rigid-body model, L is given by:

$$L = \frac{r_2}{\gamma} \tag{3.15}$$

Taking γ=0.85, h can be found from equation (4.2) as:

$$h = \sqrt[3]{\frac{12 \cdot K_1 \cdot r_2}{b \cdot E \cdot \pi \cdot 0.85^3}} \tag{3.16}$$

Assuming a thickness b=5 mm, h is found from equation (3.16) as:

h =7.6 mm (3.17)

So, after finding the link dimensions, the mechanism would like as shown in Figure 3.12.

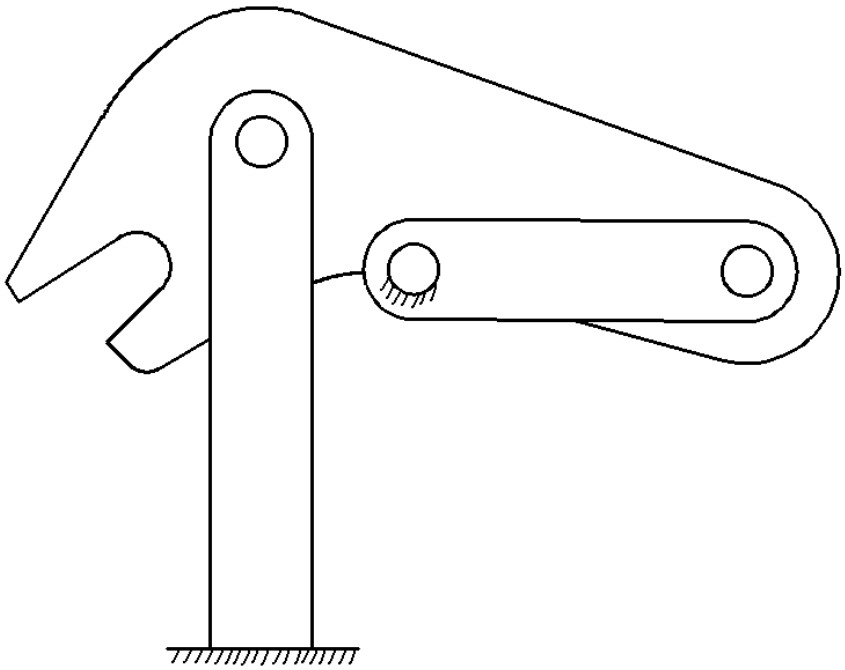

Figure 3.12: Designed compliant bistable four-bar mechanism with one torsional spring

It is important to note that position of A_o has shifted along "link 2" vector about 4.5 mm (but it is still inside the *body*'s boundary).

According to the calculated dimensions, a prototype is manufactured from a 5 mm thick Delrin plate. For the ease of manufacture, all the dimensions are multiplied

by a scale factor of 2.3 (including the width of the flexible link). Two stable positions are shown in Figure 3.13.

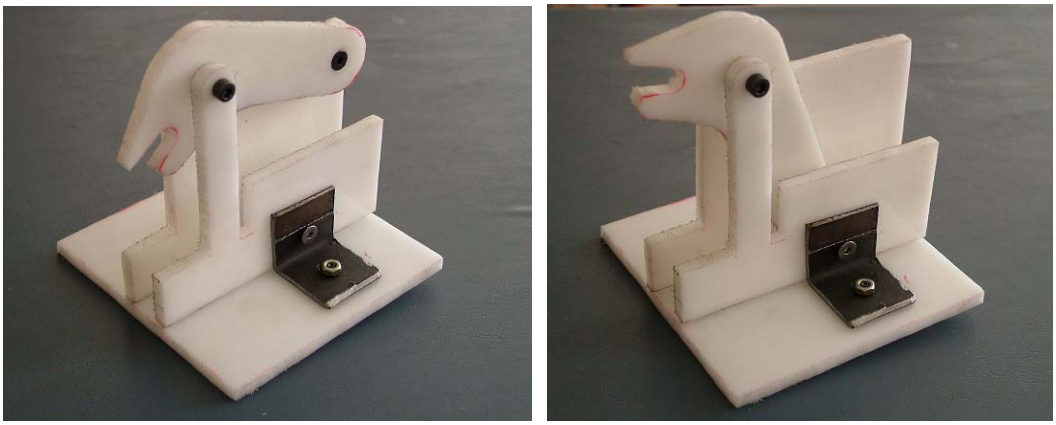

(a) (b)

Figure 3.13: Two stable positions of the prototype

Greater dimensions are introduced into the iteration routine in Appendix A and force values are calculated to be 23.3 N and 57.4 N for locking and unlocking, respectively.

In order to verify the calculated force values, measurements are taken by placing a dinamometer at the end of the beak. Measured forces between positions are 29 N and 59 N for locking and unlocking, respectively. The difference between calculated and measured values are discussed in Chapter 4.

3.3.1.7 Checking for Static Failure and Performing fatigue life analysis

In order to check for static failure and perform fatigue life analysis, maximum stress on the flexible link must be calculated first. This is done by using finite element software MSC.Marc. The mechanism modelled is shown in Figure 3.14.

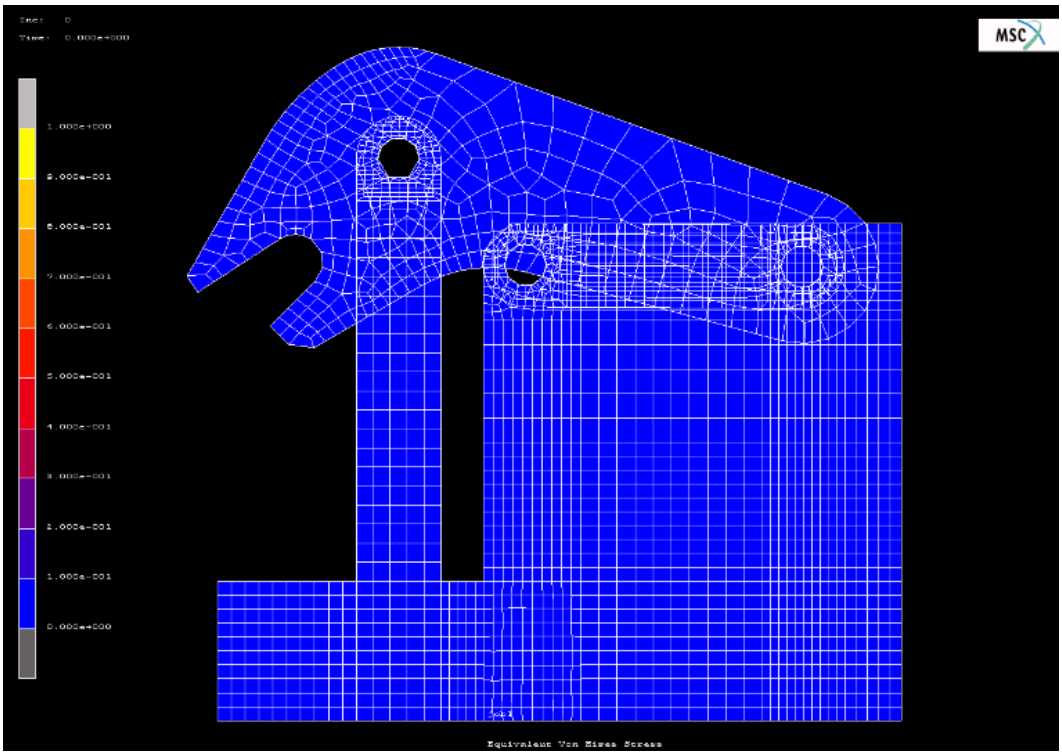

Figure 3.14: Mechanism modelled in MSC.Marc

Maximum stress occurs at the maximum deflection position, which is the unstable position of the mechanism (Figure 3.15b). Stable position, on the other hand, is the minimum stress position (Figure 3.15a).

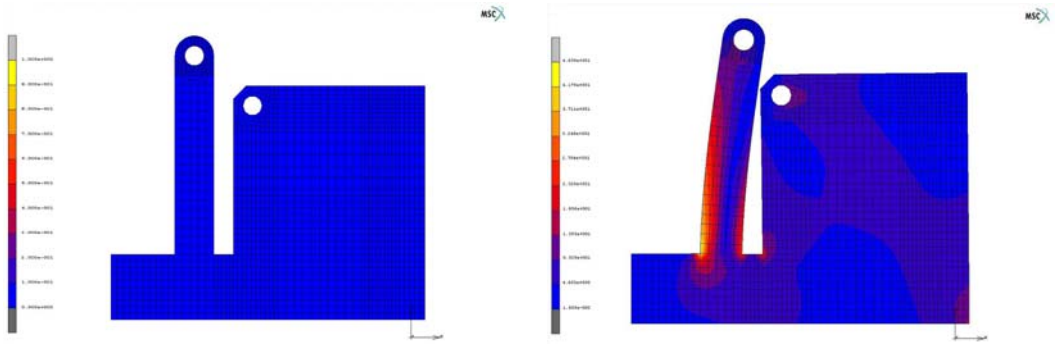

(a) (b)

Figure 3.15: Minimum and maximum stress positions of the flexible link

According to the finite element model, maximum effective stress is $\sigma' = 46{,}4$ Mpa (Figure 3.15b). Yield strength of POM is given by (Table C.1) $S_y = 60$ Mpa. So, inequality (2.15) does not hold and there is no static failure.

Fatigue life of the door lock mechanism is required to be at least 10^5 cycles, according to technical specs. Taking S_{ut}=70 Mpa (Table C.1) and putting it into equation (2.20):

$$SF = \frac{6 \cdot 70}{13 \cdot 46.4} = 0.696 \tag{3.18}$$

Value of SF=0,696 suggests a finite life for the design. Experimental life cycles can be found by looking at the S-N diagram for Delrin, shown in Figure 3.16 (dotted line shows extrusion molded Delrin, whereas intermittent line shows injection molded).

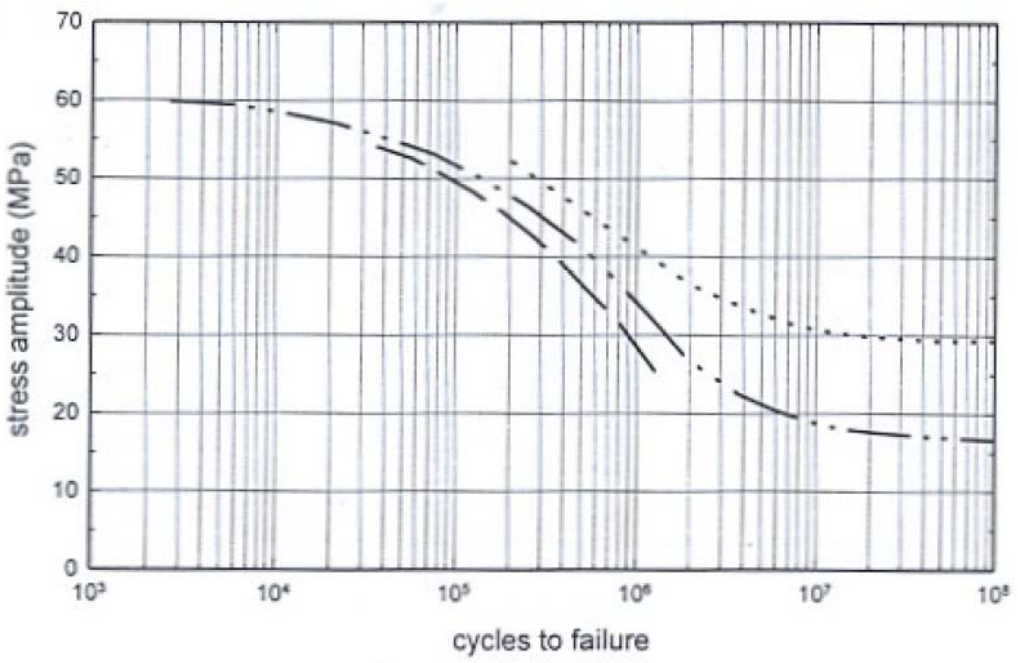

Figure 3.16: S-N diagram for extrusion and injection molded Delrin [25]

$x=3x10^5$ cycles is found. It is greater than the required value of 10^5 cycles, so the design is on the safe side when fatigue is concerned.

3.3.2 Design for several torsional springs

Unlike one torsional spring case, if the number of torsional springs are increased, bistable behaviour will depend not only on the constructed mechanism, but also the number and value of the torsional springs. So, force ratio is not only a function of coordinates of ground joint, but also a function of the value of torsional springs for this case.

Only synthesis of the mechanism in Pseudo-rigid body model form is presented in this section. The realization part has many versatilities (like different number of torsional springs, different spring locations or different segment types) and an example is presented in Appendix D.

3.3.2.1 Deciding on the two coupler joint positions

One of the stable positions of the designed mechanism will be where the flexible links or joints are undeflected. The other stable position will be where the flexible links or joints are deflected to some extent. It is a position that the forces generated on the links come to an equilibrium point. “Pole” of the *beak* cannot be chosen as one of the coupler link joints this time, since all the flexible links have to be deflected in order to reach an equilibrium.

Two coupler joints can be selected anywhere on the body. Points A and B can be chosen as the joints for the coupler link, as shown in Figure 3.16. So, the coupler link is formed with $r_3 = |AB|$.

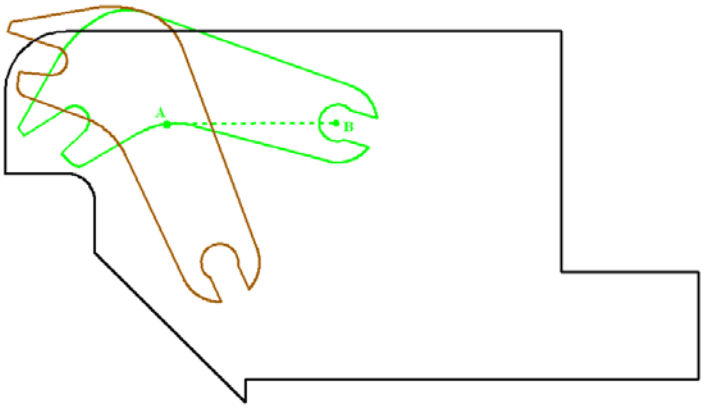

Figure 3.16: Forming the coupler link

3.3.2.2 Choosing initial position of the input link

Bistable behaviour is directly effected by the initial position, as the flexible link and joint connections are perpendicular to its connectors at the undeflected state. So different stability behaviours and force ratios can be expected for different initial positions. In fact, it would be like two completely different mechanisms.

One of the stable positions is chosen as the initial position (Figure 3.17).

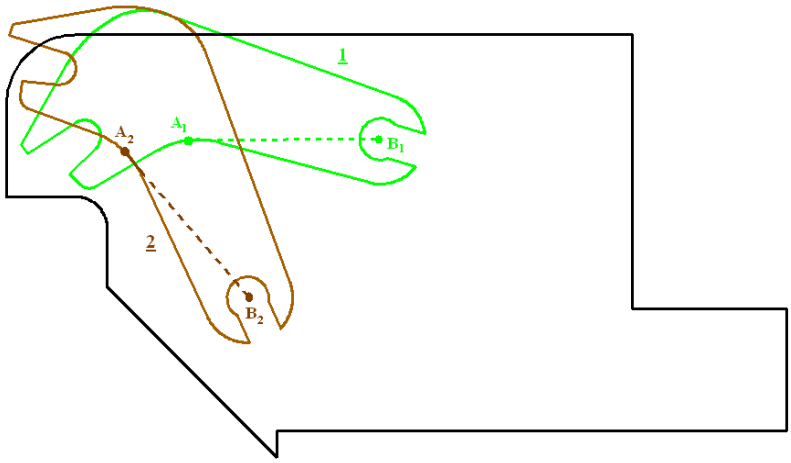

Figure 3.17: Choosing the initial position

3.3.2.3 Selecting one of the ground joint locations

Same constraint is valid again while choosing ground joint locations. Since the mechanism works in a limited area, links are limited inside the *body's* boundary. It must be remembered that, during realization of the mechanism (replacing rigid links with flexible links), link lengths will elongate, so ground joints must not be on or very near the limiting boundaries.

For the four link door lock mechanism, position of the ground joint of the second link (A_0) can be selected anywhere on the perpendicular bisector of A_1A_2. It is chosen at a position seen in Figure 3.18.

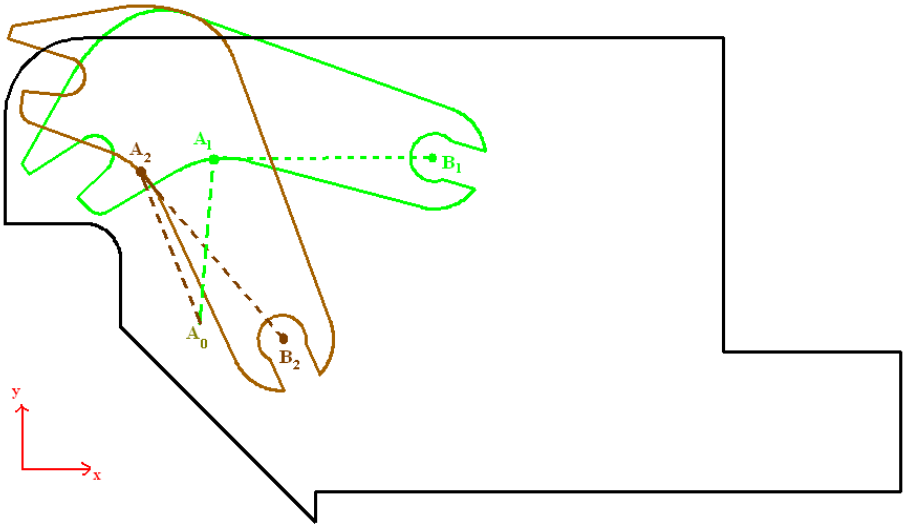

Figure 3.18: Forming the flexible link

3.3.2.4 Changing the position of the other ground joint connection

The bistable behaviour of the mechanism to be constructed is dependent on K value ratios. Combining equations (3.6) and (3.9):

$$T_3 = K_1 \cdot \psi_1 \cdot A_1 + K_2 \cdot \psi_2 \cdot (A_1 - 1) + K_3 \cdot \psi_3 \cdot (A_2 - 1) + K_4 \cdot \psi_4 \cdot A_2 \quad (3.19)$$

If K_3=K_4=0, then the equation will reduce to:

$$T_3 = K_1 \cdot \psi_1 \cdot A_1 + K_2 \cdot \psi_2 \cdot (A_1 - 1) \quad (3.20)$$

The torque value will be zero at the stable and unstable positions. But, K_1 and K_2 can't be zero or take a negative value. So, the only way to make equation (3.20) equal to zero is to search for a certain K_1/K_2 ratio that will make T_3=0 at the unstable and stable positions. This ratio can be found by evaluating the coefficients of K's throughout the motion of the constructed mechanism at the iteration point.

After finding this ratio, values of K's can be adjusted to alter maximum torque values between switching.

In order to construct a four-bar mechanism, an iteration will be made again for the other ground joint connection (B_0). When B_0 is selected; link lengths r_1 and r_4, and all angle relations can be determined. Iteration range is again the same as shown in Figure 3.8 (as point B is chosen the same as previous case).

Coupler force relation to coupler torque can be found by using free-body diagrams of the links, as shown in Figure 3.9.

A sample iteration routine for many torsional springs using Mathcad 2000 is presented in Appendix B. Using this routine, the coefficients of K's as presented in equation (3.19) are found throughout the motion of the mechanism between stable positions.

For example, if the iteration variable i=0 is chosen, the coefficient graphs will look like as shown in Figure 3.19 (coefficients are referred as C_n, where n represents the n'th torsional spring).

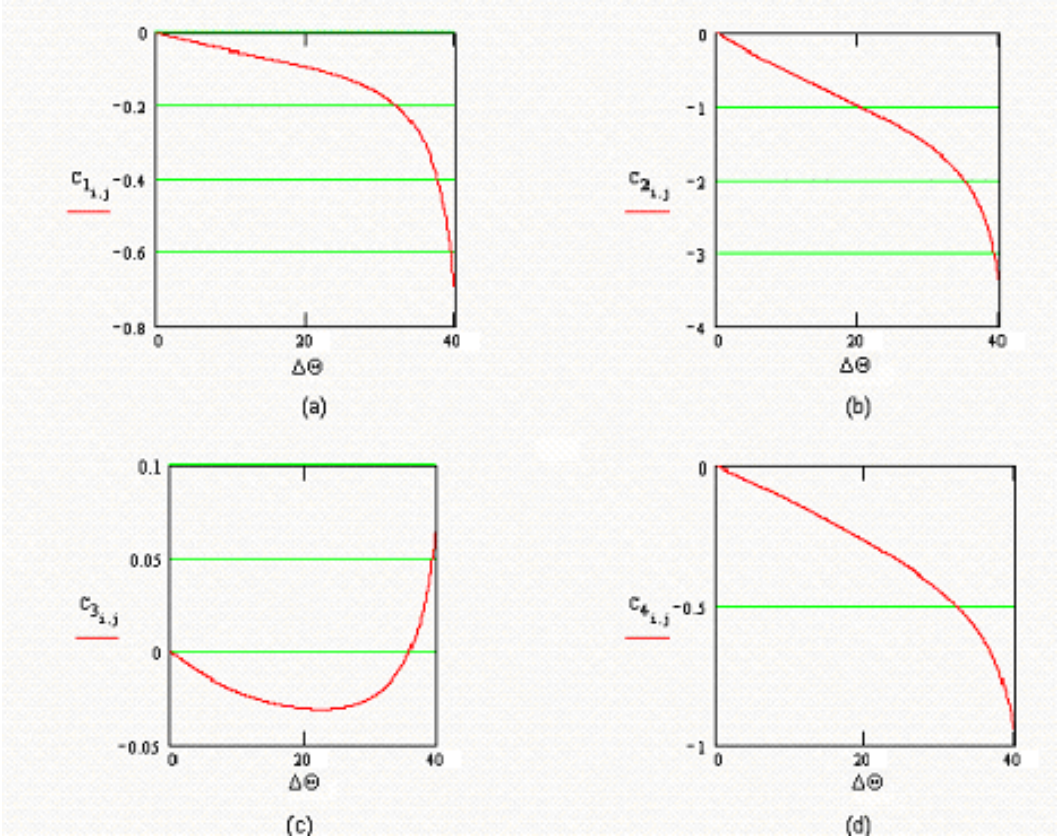

Figure 3.19: Variation of coefficients in torque equation with respect to rotation when i=0

Looking at the graph it is seen that, all the coefficient values have negative value at the end of the motion, except C_3. In order to make torque equal to zero at the end of the motion, torsional spring K_3 has to be chosen along with any other spring.

If $K_1=K_2=0$, then at the second stable position:

$$\frac{C_4}{C_3} = \frac{-0.95346}{0.66032} = -14.44 \tag{3.21}$$

Since $T_3=C_3.K_3+C_4.K_4=0$,

$$\frac{K_3}{K_4} = \frac{-C_4}{C_3} = 14.44 \tag{3.22}$$

When $K_4=1$ and $K_3=14.44$ is taken, the force versus rotation graph will look like as shown in Figure 3.20.

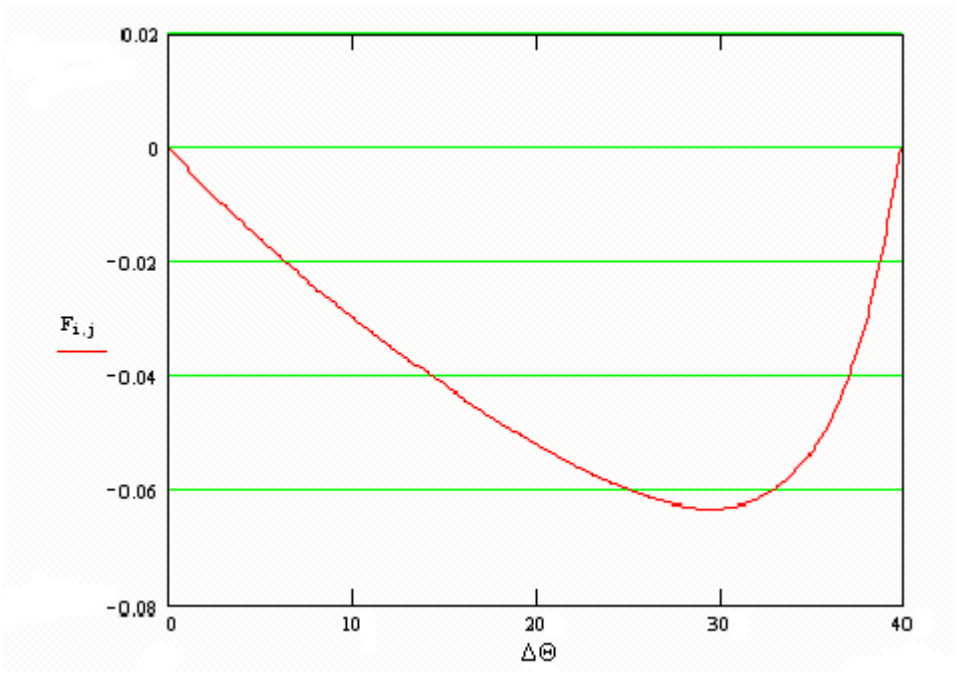

Figure 3.20: Force graph when i=0

Bistable behaviour is not reached as seen from Figure 3.20. Similar situations would occur if K_1, K_2 or both were selected not to be equal to zero. It seems that, a bistable behaviour cannot be reached when i=0.

Similarly if i=100 is chosen, coefficient values tend to go to infinity. So, i=100 cannot be selected.

Iteration for "i" goes on until a suitable position or positions are found. When i=53 is chosen, the coefficient graphs will look like as shown in Figure 3.21.

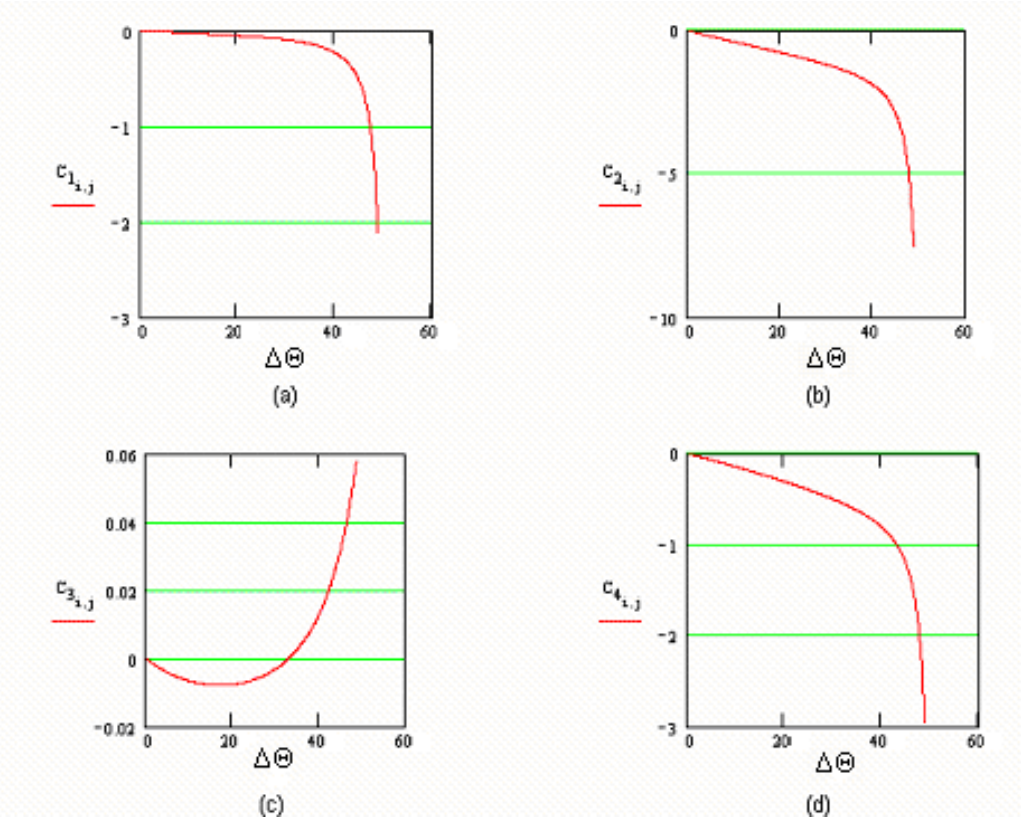

Figure 3.21: Variation of coefficients in torque equation with respect to rotation when i=53

Looking at the graphs, $K_2=K_4=0$ can be taken. So, ratio between other torsional springs is found as, $K_3/K_1=36.68$

Taking $K_1=1$ and $K_3=36.68$, the force versus rotation graph is plotted like as shown in Figure 3.22.

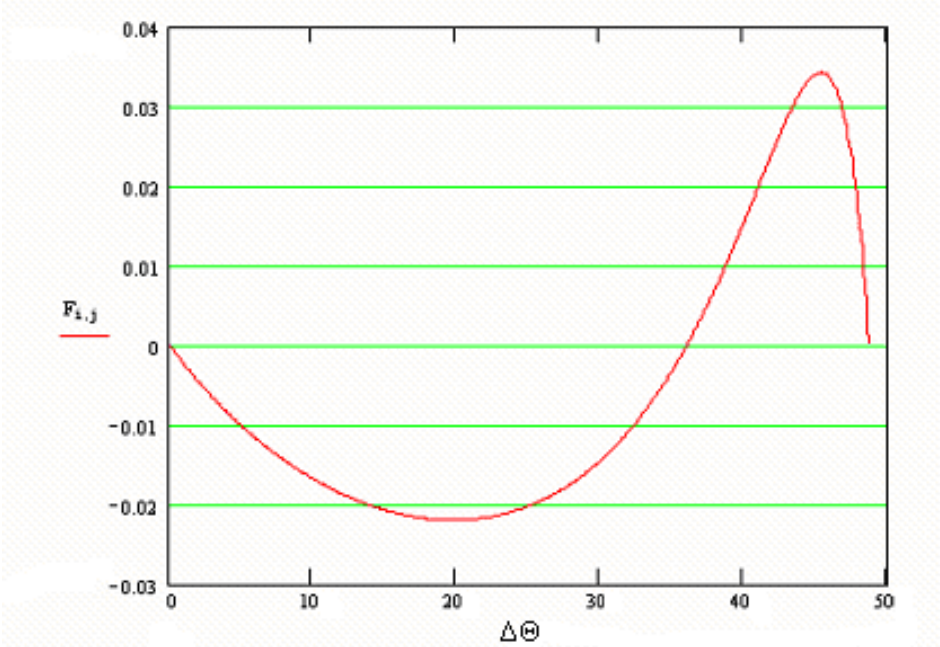

Figure 3.22: Force graph when i=53

So, bistable behaviour is reached with a force ratio of 1.56. It is an acceptable value, as it lies within tolerances as mentioned in section 3.3.1.4.

3.3.2.5 Predicting the value of the torsional spring constants

Maximum force to lock and unlock the mechanism is known in terms of K_1 and K_3. When they are taken 1 and 36.68 respectively, $F_{lock\text{-}max}$ and $F_{unlock\text{-}max}$ can be calculated as:

$F_{lock\text{-}max} = 2.2x10^{-2}$ N

$F_{unlock\text{-}max} = 3.4x10^{-2}$ N

Value of K's are directly proportional with these forces. If K_1=1300 N.mm and K_3=47700 N.mm are chosen then the forces become:

$F_{lock\text{-}max} = 28.55$ N

$F_{unlock\text{-}max} = 44.56$ N

which are acceptable according to the given force tolerances at the technical drawing shown in Figure A.1.

CHAPTER 4

DISCUSSION AND CONCLUSION

Analysis of compliant mechanisms have many difficulties, as both kinematic and deflection theory are needed. Synthesis is even harder, as many constraints are introduced. The purpose of this study was to present a design approach that can be used synthesising a compliant bistable four-link mechanism. Related work is present in literature, but the method is different in this thesis.

Pseudo-rigid body model was used to come up with a design method. Pseudo-rigid body model has the advantage that, rigid body kinematics theory is applicable on the mechanism. But, it has some limitations. Accuracy of the end coordinates of the flexible link is dependent on the position of the torsional spring and loading conditions. So, either tables for loading conditions have to be used or good assumptions have to be made. Also, there is the disadvantage that accuracy is lost at some point. But, study reveales that for many cases, end point coordinates of the flexible link is accurate for even large angles (for example, for a perpendicular force acting at the end of a flexible beam, Pseudo-rigid body model gives accurate results upto a deflection angle of 77 degrees).

A full example was also presented in this study, converting a rigid bistable mechanism into a compliant bistable mechanism. As a result, the metal spring is reduced from the mechanism. Further study can be performed on the rigid revolute joints to turn them into living hinges. Then the mechanism would be manufactured as a single piece by injection molding, which brings great advantage for serial production purposes, as the assembly time and cost would be reduced.

During the design, if torsional spring values tend to be found very large or very small, iteration must go on until a more suitable value is reached. In Chapter 3.3.1.4, iteration variable was taken to be 150 and torsional spring values were calculated accordingly. If i=100 was taken, the value of K_1 would be 250,000 N.mm in order to satisfy the force values. During the realization step, such a great torsional spring constant value would necessitate the link width to be very thick when compared to length of the link, giving the designed mechanism a clumsier look and also cause it to exceed the *body* limits. So, a range of torsional spring constants have to be considered for different materials and link dimensions, making them neither relatively large or small.

The manufactured prototype satisfies two stable positions. It has force values that is close to, but not the same as, the calculated values. The reason is that, there are thickness variations and material property variations throughout the Delrin plate and most significantly, prototype is made by hand, using a rotating saw. There are slight dimensional differences, as far as the ideal design is concerned, which created the slight differences between calculated and measured forces.

For the case of several torsional springs, only two were used as an example. But it was also possible to place three or four torsional springs. The values of the springs have to be adjusted, so that bistable behaviour is reached and force ratio is satisfied.

For the sake of convenience, some assumptions had to be made in this thesis. The position of the torsional spring (γ) for fixed-pinned link was assumed to be same for all loading conditions. The torsional spring constant coefficient ($\pi\gamma^2$) for fixed-pinned link was assumed to be same for all loading conditions. But this design approach using Pseudo-rigid body model has proved itself very useful. The prototype that has been designed using the theory, has fulfilled the design requirements.

The finite element model has been made by Bias Enginnering Company. Since the thickness is relatively small, 2-D plane stress elements are used. These elements are quadratic elements with four nodes. For the boundary conditions, flexible link is fixed to the ground and displacement is introduced at the tip of the beak, until the flexible link reaches its maximum deflection position.

The finite element model of the flexible link has sharp edges and corners. In real life, there should be a radius at the corners for manufacturing purposes. It is possible to add a radius at the corners (where stress is maximum) and check the results. Figure 4.1 (a) shows a finite element model with radius and increased number of elements. Figure 4.1 (b) shows the stress variation at the maximum deflection position. Results are similar, except that maximum stress is increased about 3 Mpa. This model still satisfies static and fatigue failure requirements.

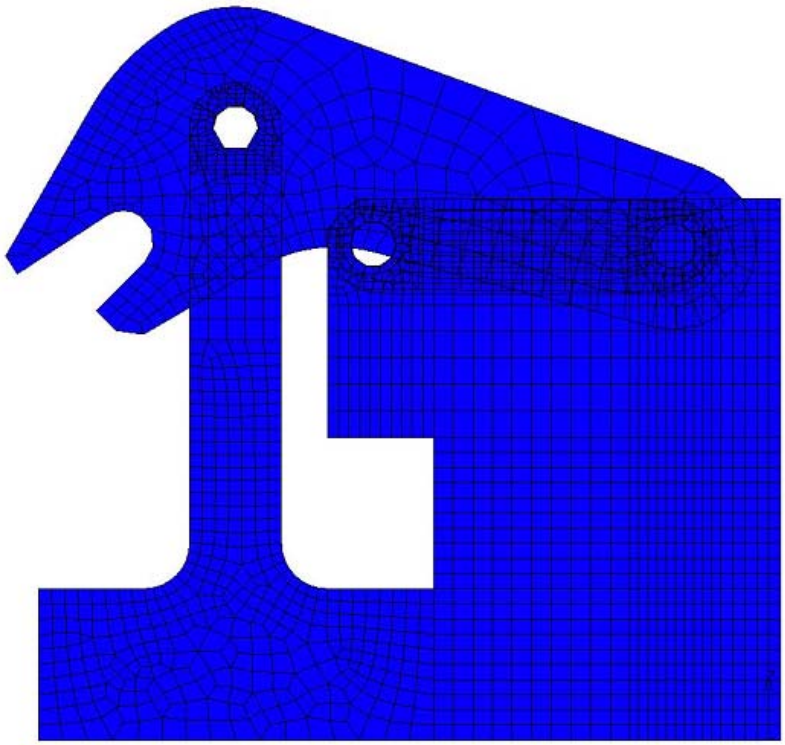

Figure 4.1 (a): Finite element model of the mechanism with radius at the corner

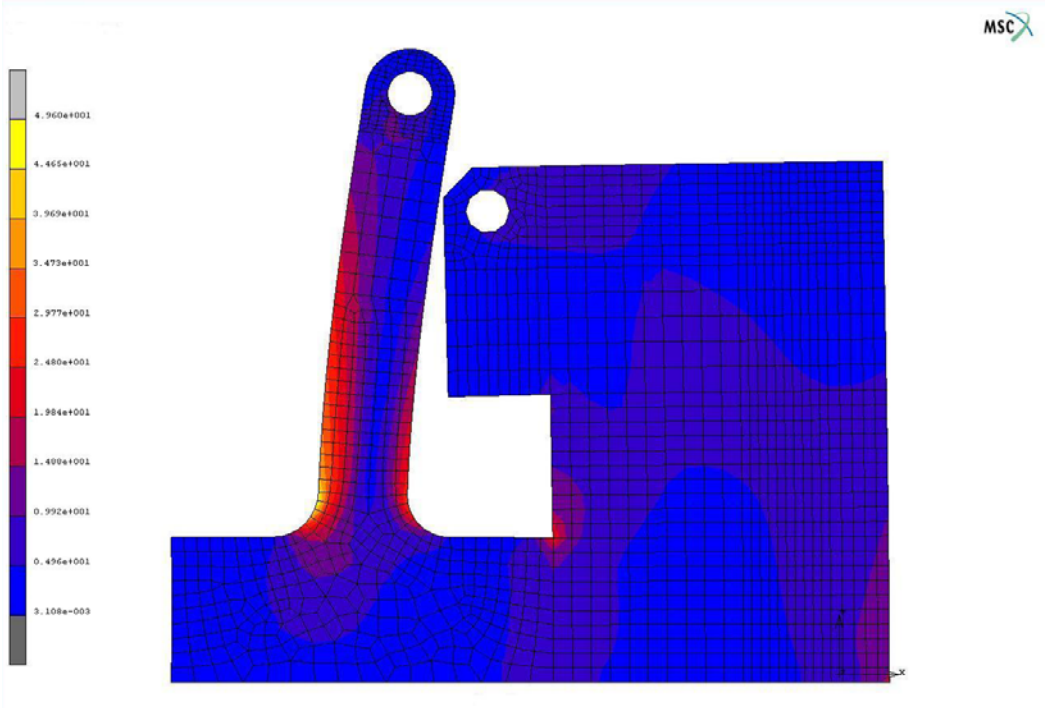

Figure 4.1 (b): Stress variation at the maximum deflected position

As a future work, a design software using the principals presented in this thesis can be developed. Living hinges are important to design a fully compliant bistable mechanism, so related work about their design method and fatigue life can be performed (work about living hinges in literature are limited and mostly experimental). Also, a similar design approach can be developed for other kind of mechanisms or for other purposes again using Pseudo-rigid body model.

REFERENCES

1. Frecker, Mary I., Canfield, Shawn, Methodology for Systematic Design of Compliant Mechanisms with Integrated Smart Materials.

2. Howell, Larry L., Compliant Mechanisms, John Wiley & Sons Inc., 2001

3. Jensen, Brian D., Identification of Macro and Micro Compliant Mechanism Configurations Resulting In Bistable Behaviour, M.S., Brigham Young University, 1998

4. Jensen, Brian D., Howell, Larry L., Salmon, Linton G., Introduction Of Two-link, In-plane, Bistable Compliant MEMS, ASME Design Engineering Technical Conferences, September 13-16, 1998

5. Jensen, Brian D., Parkinson, Matthew B., Kurabayashi, Katsuo, Howell, Larry L., Baker, Michael S., Design Optimization Of A Fully Compliant Bistable Micro Mechanism, ASME International Mechanical Engineering Congress and Exposition, November 11-16, 2001

6. Jensen, Brian D., Howell, Larry L., Roach, Gregory M., Bistable Compliant Mechanism, United States Patent, Patent No: US 6,215,081 B1, 2001

7. Kota, Sridhar, Joo, Jinyong, Li Zhe, Rodgers, Steven M., Sniegowski, Jeff, Design of Compliant Mechanisms: Application to MEMS, Kluwer Academic Publishers, 2001

8. Opdahl, Patrick G., Jensen, Brian D., Howell, Larry L., An Investigation Into Compliant Bistable Mechanisms, ASME Design Engineering Technical Conferences, September 13-16, 1998

9. Parkinson, Matthew B., Jensen, Brian D., Roach, Gregory M., Optimization Based Design Of A Fully Compliant Bistable Micromechanism, ASME Design Engineering Technical Conferences, September 10-13, 2000

10. Shames, Irving H., Engineering Mechanics (3rd Edition), Prentice-Hall Inc., 1980

11. Shigley, J.Edward, Mechanical Engineering Design (First Metric Edition), McGraw Hill, 1986

12. Sevak, N.M., McLarnen, C.W., Optimal Synthesis of Flexible Link Mechanisms with Large Static Deflections, ASME Paper, 1974

13. Soylu, R., ME 301-Theory of Machines class notes, Middle East Technical University, 2000

14. Söylemez, E., Mechanisms (3rd Edition), Middle East Technical University, Publication Number: 64, 1999

15. Söylemez, E., ME 431-Synthesis of Mechanisms class notes, Middle East Technical University, 2001

16. Wittwer, Jonathan W., Predicting the Effects of Dimensional and Material Property Variations in Micro Compliant Mechanisms, M.S., Brigham Young University, 2001

17. Kota, Sridhar, Compliant Systems Design Laboratory, www.engin.umich.edu/labs/csdl/app.html, 2005

18. Flexsys Inc., Automotive Windshield Wiper, www.flxsys.com/wiper-blade_pic-proto.shtml, 2005

19. Howell, Larry L., Compliant Mechanisms Home Page at Byu, www.research.et.byu.edu/llhwww/, 2005

20. Pedersen, Claus B.W., Buhl, Thomas, Topology Optimization, www.topopt.dtu.dk/Theory1, 2005

21. MSC Software, ADAMS/Autoflex, www.mscsoftware.com/Products/Products_Detail.cfm?PI=423&S=91, 2005

22. Anantashuresh, G.K., The research Group of Anantashuresh, www.seas.upenn.edu/~gksuresh/mysoft.html, 2005

23. Quint Corporation, OPTISHAPE, www.quint.co.jp/eng/pro/ots/index.htm, 2005

24. Arcelik "Malbis" Material Database, 2005

25. Plastic Design Library Staff, Fatigue and Tribological Properties of Plastics and Elastomers, 1995

APPENDIX A

ITERATION ROUTINE IN MATHCAD FOR ONE K

Choosing the position of the fourth link********

$i := 0$ => **x** coordinate of Bo that is to be changed between 0 and 577

$$B_{0y_i} := -0.83891 \cdot \frac{i - 59}{10} + 25.79947$$ => **y** coordinate of Bo is found by equation (2.4)

$$r_{1_i} := \sqrt{\left(\frac{i - 59}{10}\right)^2 + \left(B_{0y_i}\right)^2}$$

$r_2 := 25.8$

$r_3 := 30$

$$r_{4_i} := \sqrt{\left[\left(\frac{i - 59}{10}\right) - 28.98\right]^2 + \left(B_{0y_i} - 18.04\right)^2}$$

=> unknown link lengths are calculated with respect to variable **i**

$$c\theta 1_i := \frac{\left(\frac{i - 59}{10}\right)}{r_{1_i}} \qquad s\theta 1_i := \frac{B_{0y_i}}{r_{1_i}} \qquad c\theta 40i_i := \frac{28.98 - \left(\frac{i - 59}{10}\right)}{r_{4_i}} \qquad s\theta 40i_i := \frac{B_{0y_i} - 18.04}{r_{4_i}}$$

$$\theta 1_i := \operatorname{atan2}\left(c\theta 1_i, s\theta 1_i\right) \qquad \theta 40_i := -\operatorname{atan2}\left(c\theta 40i_i, s\theta 40i_i\right)$$

$\theta 40_i := \theta 40i_i - \theta 1_i$ => initial position of the link to be rotated is calculated with respect to link 1

Freudenstein equations********

$a := 25.357$

$$\text{interval}_i := \operatorname{acos}\left[\frac{2 \cdot \left(r_{4_i}\right)^2 - a^2}{2 \cdot \left(r_{4_i}\right)^2}\right]$$

$$M_i := \operatorname{trunc}\left(10 \text{interval}_i \cdot \frac{180}{\pi}\right)$$

$j := 0 .. M_i$

$$\theta 4_{i,j} := \text{if}\left(i < 267, \theta 40_i \cdot \frac{180}{\pi} - \frac{j}{10}, \theta 40_i \cdot \frac{180}{\pi} + \frac{j}{10}\right)$$

=> Input link is rotated between stable positions

$$k_{1_i} := \frac{\left[\left(r_{4_i}\right)^2 + \left(r_{1_i}\right)^2 - r_2^{\,2} + r_3^{\,2}\right]}{2 \cdot r_{4_i} \cdot r_3} \qquad k_{2_i} := \frac{r_{1_i}}{r_{4_i}} \qquad k_{3_i} := \frac{r_{1_i}}{r_3}$$

$$A_{i,j} := \cos\left(\theta_{4_{i,j}} \cdot \frac{\pi}{180}\right) + k_{2_i} \qquad B_{i,j} := \sin\left(\theta_{4_{i,j}} \cdot \frac{\pi}{180}\right) \qquad C_{i,j} := k_{3_i} \cdot \cos\left(\theta_{4_{i,j}} \cdot \frac{\pi}{180}\right) + k_{1_i}$$

$$t_{i,j} := \frac{B_{i,j} - \sqrt[2]{\left(B_{i,j}\right)^2 - \left(C_{i,j}\right)^2 + \left(A_{i,j}\right)^2}}{C_{i,j} + A_{i,j}}$$

$$c_{3_{i,j}} := \frac{1 - \left(t_{i,j}\right)^2}{1 + \left(t_{i,j}\right)^2} \qquad s_{3_{i,j}} := \frac{2 \cdot t_{i,j}}{1 + \left(t_{i,j}\right)^2}$$

$\theta_{3_{i,j}} := \operatorname{atan2}\left(c_{3_{i,j}}, s_{3_{i,j}}\right)$ => angle of the third link is calculated throughout the motion

$$c_{2_{i,j}} := \frac{\left(-r_3 \cdot \cos\left(\theta_{3_{i,j}}\right) + r_{4_i} \cdot \cos\left(\theta_{4_{i,j}} \cdot \frac{\pi}{180}\right) + r_{1_i}\right)}{r_2} \qquad s_{2_{i,j}} := \frac{\left(-r_3 \cdot \sin\left(\theta_{3_{i,j}}\right) + r_{4_i} \cdot \sin\left(\theta_{4_{i,j}} \cdot \frac{\pi}{180}\right)\right)}{r_2}$$

$\theta_{2_{i,j}} := \operatorname{atan2}\left(c_{2_{i,j}}, s_{2_{i,j}}\right)$ => angle of the second link is calculated throughout the motion

Potential energy equations

$$\psi_{1_{i,j}} := \left(\theta_{2_{i,j}} - \theta_{2_{i,0}}\right)$$

$$A_{1_{i,j}} := \frac{r_3 \cdot \sin\left(\theta_{3_{i,j}} - \theta_{4_{i,j}} \cdot \frac{\pi}{180}\right)}{r_2 \cdot \sin\left(\theta_{4_{i,j}} \cdot \frac{\pi}{180} - \theta_{2_{i,j}}\right)}$$

$K_1 := 1$ => torsional spring constant value

$T_{i,j} := K_1 \cdot \psi_{1_{i,j}} \cdot A_{1_{i,j}}$ => input torque (torque on link 3)

Force calculations********

$$x_{i,j} := 12.1 + r_2 \cdot \cos\left(\theta 1_i + \theta 2_{i,j}\right)$$

$$det_{i,j} := \begin{vmatrix} -r_2 \cdot \sin\left(\theta 2_{i,j}\right) & r_2 \cdot \cos\left(\theta 2_{i,j}\right) & 0 & 0 & 0 \\ 0 & 0 & -r4_i \cdot \sin\left(\theta 4_{i,j} \cdot \frac{\pi}{180}\right) & r4_i \cdot \cos\left(\theta 4_{i,j} \cdot \frac{\pi}{180}\right) & 0 \\ -1 & 0 & -1 & 0 & \cos\left(\frac{\pi}{2} - \theta 1_i\right) \\ 0 & -1 & 0 & -1 & \sin\left(\frac{\pi}{2} - \theta 1_i\right) \\ 0 & 0 & r_3 \cdot \sin\left(\theta 3_{i,j}\right) & -r_3 \cdot \cos\left(\theta 3_{i,j}\right) & -x_{i,j} \end{vmatrix}$$

Cramer's rule is applied to predict the force:

$$F_{i,j} := \frac{\begin{vmatrix} -r_2 \cdot \sin\left(\theta 2_{i,j}\right) & r_2 \cdot \cos\left(\theta 2_{i,j}\right) & 0 & 0 & 0 \\ 0 & 0 & -r4_i \cdot \sin\left(\theta 4_{i,j} \cdot \frac{\pi}{180}\right) & r4_i \cdot \cos\left(\theta 4_{i,j} \cdot \frac{\pi}{180}\right) & 0 \\ -1 & 0 & -1 & 0 & 0 \\ 0 & -1 & 0 & -1 & 0 \\ 0 & 0 & r_3 \cdot \sin\left(\theta 3_{i,j}\right) & -r_3 \cdot \cos\left(\theta 3_{i,j}\right) & -T_{i,j} \end{vmatrix}}{det_{i,j}}$$

Force versus rotation graph:

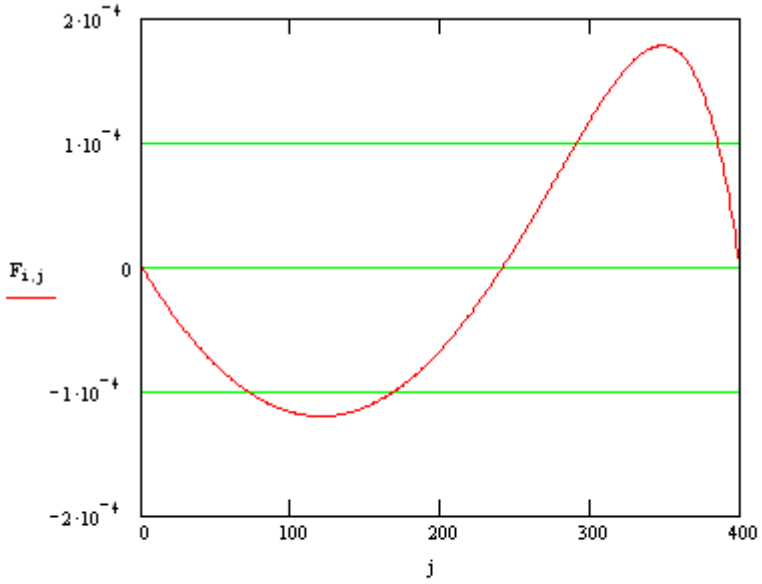

$P_j := F_{i,j}$

$$ratio := if\left(\left|min(P)\right| > max(P), \frac{min(P)}{max(P)}, \frac{max(P)}{min(P)}\right)$$

$ratio = -1.48001$

APPENDIX B

ITERATION ROUTINE IN MATHCAD FOR SEVERAL K

Choosing the position of the fourth link********

$i := 53$ => **x** coordinate of Bo that is to be changed between 0 and 577

$$B_{0y_i} := -0.8391 \cdot \frac{i - 99}{10} + 22.4676$$ => **y** coordinate of Bo is found by equation (2.4)

$$r1_i := \sqrt{\left(\frac{i - 99}{10}\right)^2 + \left(B_{0y_i}\right)^2}$$

$r_2 := 17.95$

$r_3 := 23.7$

$$r4_i := \sqrt{\left[\left(\frac{i - 99}{10}\right) - 25.01\right]^2 + \left(B_{0y_i} - 18.04\right)^2}$$

=> unknown link lengths are calculated with respect to variable **i**

$$c\theta 1_i := \frac{\left(\frac{i - 99}{10}\right)}{r1_i} \qquad s\theta 1_i := \frac{B_{0y_i}}{r1_i} \qquad c\theta 40i_i := \frac{25.01 - \left(\frac{i - 99}{10}\right)}{r4_i} \qquad s\theta 40i_i := \frac{B_{0y_i} - 18.04}{r4_i}$$

$$\theta 1_i := \operatorname{atan2}\left(c\theta 1_i, s\theta 1_i\right) \qquad \theta 40i_i := -\operatorname{atan2}\left(c\theta 40i_i, s\theta 40i_i\right)$$

$$\theta 40_i := \theta 40i_i - \theta 1_i$$ => initial position of the link to be rotated is calculated with respect to link 1

Freudenstein equations********

$a := 25.357$

$$\text{interval}_i := \operatorname{acos}\left[\frac{2 \cdot \left(r4_i\right)^2 - a^2}{2 \cdot \left(r4_i\right)^2}\right]$$

$$M_i := \operatorname{trunc}\left(10 \,\text{interval}_i \cdot \frac{180}{\pi}\right)$$

$j := 0 .. M_i$

$$\theta 4_{i,j} := \text{if}\left(i < 267, \theta 40_i \cdot \frac{180}{\pi} - \frac{j}{10}, \theta 40_i \cdot \frac{180}{\pi} + \frac{j}{10}\right)$$

=> Input link is rotated between stable positions

$$k_{1_i} := \frac{\left[\left(r_{4_i}\right)^2 + \left(r_{1_i}\right)^2 - r_2^{\,2} + r_3^{\,2}\right]}{2 \cdot r_{4_i} \cdot r_3} \qquad k_{2_i} := \frac{r_{1_i}}{r_{4_i}} \qquad k_{3_i} := \frac{r_{1_i}}{r_3}$$

$$A_{i,j} := \cos\left(\theta_{4_{i,j}} \cdot \frac{\pi}{180}\right) + k_{2_i} \qquad B_{i,j} := \sin\left(\theta_{4_{i,j}} \cdot \frac{\pi}{180}\right) \qquad C_{i,j} := k_{3_i} \cdot \cos\left(\theta_{4_{i,j}} \cdot \frac{\pi}{180}\right) + k_{1_i}$$

$$t_{i,j} := \frac{B_{i,j} - \sqrt[2]{\left(B_{i,j}\right)^2 - \left(C_{i,j}\right)^2 + \left(A_{i,j}\right)^2}}{C_{i,j} + A_{i,j}}$$

$$c_{3_{i,j}} := \frac{1 - \left(t_{i,j}\right)^2}{1 + \left(t_{i,j}\right)^2} \qquad s_{3_{i,j}} := \frac{2 \cdot t_{i,j}}{1 + \left(t_{i,j}\right)^2}$$

$$\theta_{3_{i,j}} := \operatorname{atan2}\left(c_{3_{i,j}}, s_{3_{i,j}}\right)$$

=> angle of the third link is calculated throughout the motion

$$c_{2_{i,j}} := \frac{\left(-r_3 \cdot \cos\left(\theta_{3_{i,j}}\right) + r_{4_i} \cdot \cos\left(\theta_{4_{i,j}} \cdot \frac{\pi}{180}\right) + r_{1_i}\right)}{r_2} \qquad s_{2_{i,j}} := \frac{\left(-r_3 \cdot \sin\left(\theta_{3_{i,j}}\right) + r_{4_i} \cdot \sin\left(\theta_{4_{i,j}} \cdot \frac{\pi}{180}\right)\right)}{r_2}$$

$$\theta_{2_{i,j}} := \operatorname{atan2}\left(c_{2_{i,j}}, s_{2_{i,j}}\right)$$

=> angle of the second link is calculated throughout the motion

Potential energy equations

$$\psi_{1_{i,j}} := \left(\theta_{2_{i,j}} - \theta_{2_{i,0}}\right) \qquad \psi_{2_{i,j}} := \left(\theta_{2_{i,j}} - \theta_{2_{i,0}}\right) - \left(\theta_{3_{i,j}} - \theta_{3_{i,0}}\right)$$

$$\psi_{4_{i,j}} := \left(\theta_{4_{i,j}} - \theta_{4_{i,0}}\right) \cdot \frac{\pi}{180} \qquad \psi_{3_{i,j}} := \left(\theta_{4_{i,j}} - \theta_{4_{i,0}}\right) \cdot \frac{\pi}{180} - \left(\theta_{3_{i,j}} - \theta_{3_{i,0}}\right)$$

$$A_{1_{i,j}} := \frac{r_3 \cdot \sin\left(\theta_{3_{i,j}} - \theta_{4_{i,j}} \cdot \frac{\pi}{180}\right)}{r_2 \cdot \sin\left(\theta_{4_{i,j}} \cdot \frac{\pi}{180} - \theta_{2_{i,j}}\right)} \qquad A_{2_{i,j}} := \frac{r_3 \cdot \sin\left(\theta_{3_{i,j}} - \theta_{2_{i,j}}\right)}{r_{4_i} \cdot \sin\left(\theta_{4_{i,j}} \cdot \frac{\pi}{180} - \theta_{2_{i,j}}\right)}$$

$K_1 := 1 \qquad K_2 := 0 \qquad K_3 := 36.68 \qquad K_4 := 0$ => torsional spring constant values

Input torque (torque on link 3):

$$T_{i,j} := K_1 \cdot \psi 1_{i,j} \cdot A1_{i,j} + K_2 \cdot \psi 2_{i,j} \cdot \left(A1_{i,j} - 1\right) + K_3 \cdot \psi 3_{i,j} \cdot \left(A2_{i,j} - 1\right) + K_4 \cdot \psi 4_{i,j} \cdot A2_{i,j}$$

Coefficient graphs of the torsional spring constants in the torque equation:

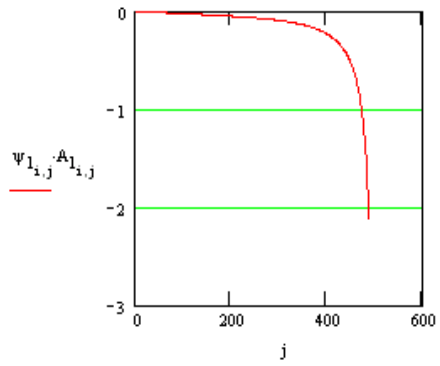

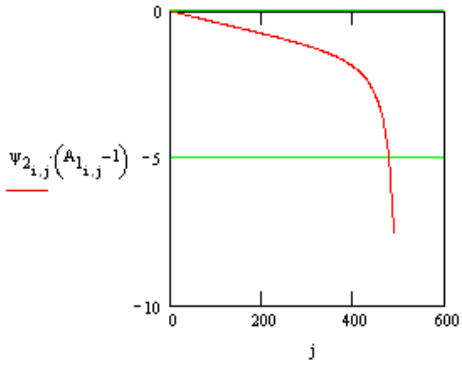

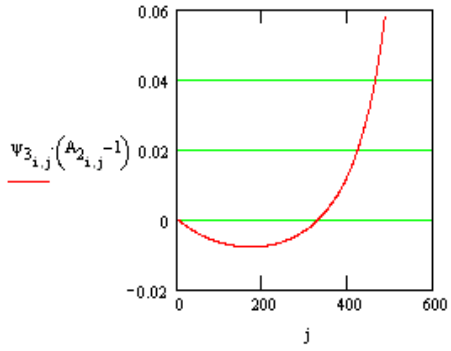

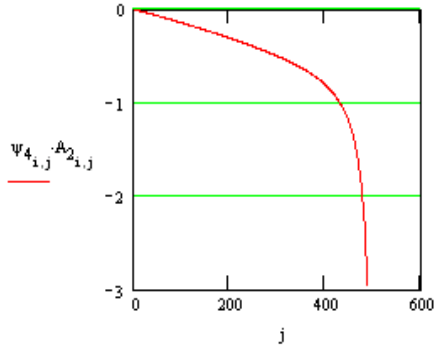

Force calculations

$$x_{i,j} := 16.07 + r_2 \cdot \cos\left(\theta 1_i + \theta 2_{i,j}\right)$$

$$det_{i,j} := \begin{vmatrix} -r_2 \cdot \sin\left(\theta 2_{i,j}\right) & r_2 \cdot \cos\left(\theta 2_{i,j}\right) & 0 & 0 & 0 \\ 0 & 0 & -r4_i \cdot \sin\left(\theta 4_{i,j} \cdot \frac{\pi}{180}\right) & r4_i \cdot \cos\left(\theta 4_{i,j} \cdot \frac{\pi}{180}\right) & 0 \\ -1 & 0 & -1 & 0 & \cos\left(\frac{\pi}{2} - \theta 1_i\right) \\ 0 & -1 & 0 & -1 & \sin\left(\frac{\pi}{2} - \theta 1_i\right) \\ 0 & 0 & r_3 \cdot \sin\left(\theta 3_{i,j}\right) & -r_3 \cdot \cos\left(\theta 3_{i,j}\right) & x_{i,j} \end{vmatrix}$$

Cramer's rule is applied to predict the force:

$$F_{i,j} := \frac{\left|\begin{pmatrix} -r_2 \cdot \sin\left(\theta 2_{i,j}\right) & r_2 \cdot \cos\left(\theta 2_{i,j}\right) & 0 & 0 & 0 \\ 0 & 0 & -r4_i \cdot \sin\left(\theta 4_{i,j} \cdot \frac{\pi}{180}\right) & r4_i \cdot \cos\left(\theta 4_{i,j} \cdot \frac{\pi}{180}\right) & 0 \\ -1 & 0 & -1 & 0 & 0 \\ 0 & -1 & 0 & -1 & 0 \\ 0 & 0 & r_3 \cdot \sin\left(\theta 3_{i,j}\right) & -r_3 \cdot \cos\left(\theta 3_{i,j}\right) & T_{i,j} \end{pmatrix}\right|}{det_{i,j}}$$

Force versus rotation graph:

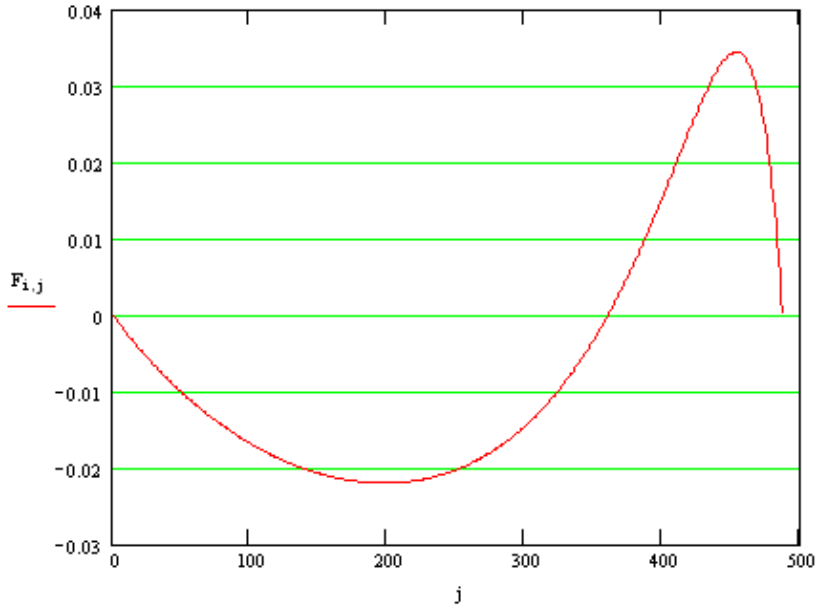

$P_j := F_{i,j}$

$$ratio := if\left(\left|min(P)\right| > max(P), \frac{min(P)}{max(P)}, \frac{max(P)}{min(P)}\right)$$

ratio = −1.5649679

APPENDIX C

MECHANICAL PROPERTIES OF SOME POLYMERS

Table C.1: Mechanical properties of some polymers [2], [11], [24]

Material	Property	Flexural Modulus (Mpa)	Yield Stregth (Mpa)	Ultimate Tensile Stregth (Mpa)
POLYSTREN	Extrusion	1400	15	-
	Injection moldeable gpps	2500	40	80
	Injection moldeable hips	1200	15	-
	Injection moldeable high glass hips	1800	20	-
ABS	Extrusion	2000	30	55
	Injection moldeable	-	40	55
POLYETHYLEN	High density	-	20	
POLYPROPYLENE	Homopolymer	1400	30	40
	Copolymer	1200	25	40
	%20 material filled injection moldeable	2300	25	40
	%40 material filled injection moldeable	3200	25	40
	Glass fiber reinforced	6000	75	-
POM	Injection moldeable	2300	60	70
PVC	Extrusion	-	30	-
POLYIMIDE	Polyamide 6 without filler	2800	75	-
	Polyamide 6 %30-35 glass reinforced	8200	178	-
	Polyamide 6,6 without filler	3000	80	-
	Polyamide 6,6 %10-15 glass reinforced	4800	100	-
	Polyamide 6,6 %20-25 glass reinforced	5300	120	-
	Polyamide 6,6 %30-35 glass reinforced	8900	185	340
PMMA	Injection moldeable	-	60	-
PC	Injection moldeable	-	60	110
PBT	Without filler	2700	50	-
	%10-15 glass reinforced	6000	95	-

APPENDIX D

AN EXAMPLE OF A COMPLIANT MECHANISM FOR THE CASE OF MANY TORSIONAL SPRINGS

For the constructed door lock mechanism, K_1 can be chosen as a fixed-pinned link and K_3 might be a small-length-flexural pivot. Assuming a rectangular cross-section for K_1, and taking E=2300 Mpa, b=5 mm, from equations (3.14), (3.15) and (3.16): h = 2.3 mm

Similarly for K_3, equation (2.11) can be used. Assuming a rectangular cross-section and taking E=2300 Mpa, b=5 mm, ℓ=4 mm: h = 5.8 mm

After finding the link dimensions, the mechanism would have two possible configurations as shown in Figure D.1 (a) and (b).

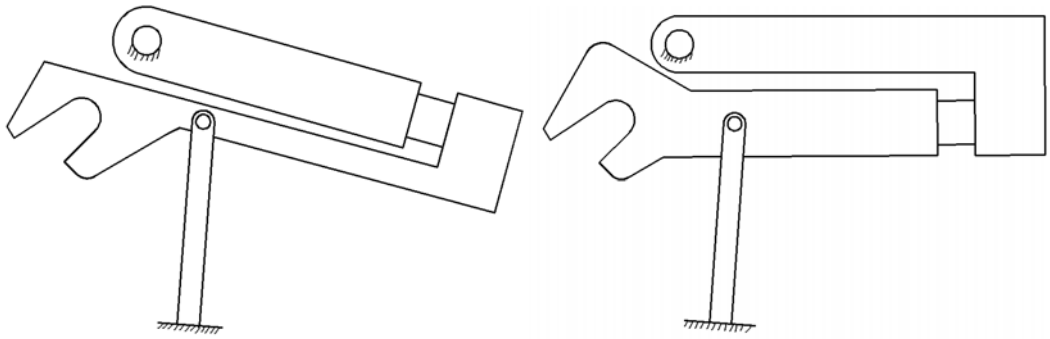

(a) (b)

Figure D.1: Designed compliant bistable four-bar mechanism with two torsional springs

The fatigue life expectancy can be calculated similarly as presented in Chapter 3.3.1.7.